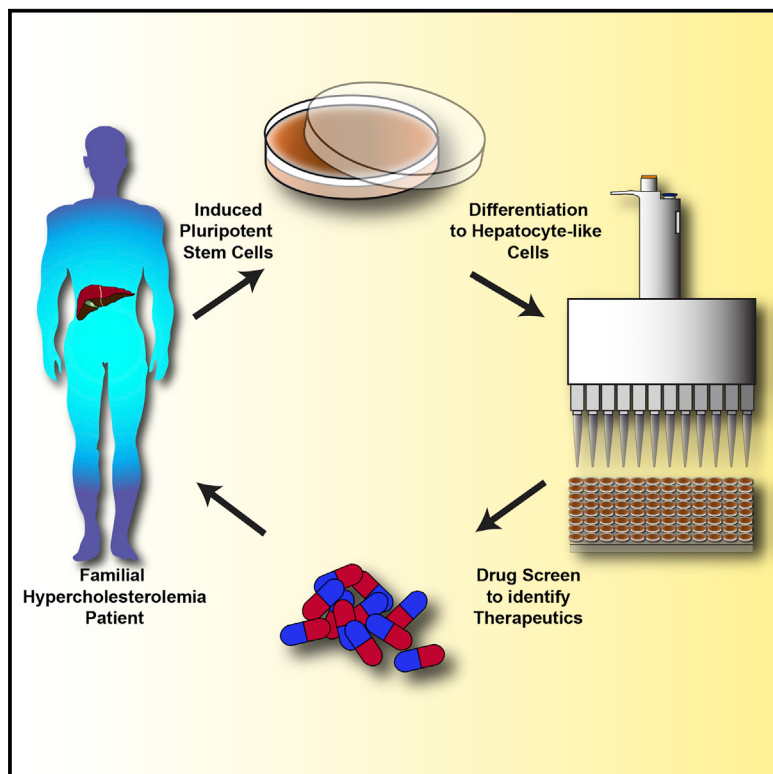


A Drug Screen using Human iPSC-Derived Hepatocyte-like Cells Reveals Cardiac Glycosides as a Potential Treatment for Hypercholesterolemia

Graphical Abstract



Authors

Max A. Cayo, Sunil K. Mallanna,
Francesca Di Furio, ...,
Markus Grompe, Daniel J. Rader,
Stephen A. Duncan

Correspondence

duncanst@musc.edu

In Brief

Cayo et al. of the NHLBI NextGen consortium use hepatocytes from familial hypercholesterolemia iPSCs in a drug screen that highlights cardiac glycosides as a candidate treatment acting to reduce apoB levels via proteolytic turnover and as a result lower LDL-C.

Highlights

- HoFH iPSC-derived hepatocytes provide a platform to identify LDL-C-lowering drugs
- Screening reveals that cardiac glycosides can reduce hepatocyte production of apoB
- ApoB reduction occurs via increased proteolytic turnover
- Cardiac glycoside treatment reduces serum LDL-C in patients and humanized mice

A Drug Screen using Human iPSC-Derived Hepatocyte-like Cells Reveals Cardiac Glycosides as a Potential Treatment for Hypercholesterolemia

Max A. Cayo,¹ Sunil K. Mallanna,² Francesca Di Furio,² Ran Jing,² Lauren B. Tolliver,² Matthew Bures,¹ Amanda Urick,^{1,2} Fallon K. Noto,¹ Evanthia E. Pashos,³ Matthew D. Greseth,⁴ Maciej Czarnecki,^{4,5} Paula Traktman,^{4,6,7} Wenli Yang,⁸ Edward E. Morrisey,⁸ Markus Grompe,⁹ Daniel J. Rader,³ and Stephen A. Duncan^{1,2,7,10,*}

¹Department of Cell Biology, Neurobiology, and Anatomy, Medical College of Wisconsin, 8701 Watertown Plank Road, Milwaukee, WI 53226, USA

²Department of Regenerative Medicine and Cell Biology, Medical University of South Carolina, 173 Ashley Avenue, Charleston, SC 29425, USA

³Departments of Medicine and Genetics and the Institute for Translational Medicine and Therapeutics, Perelman School of Medicine, University of Pennsylvania, Philadelphia, PA 19104, USA

⁴Department of Microbiology and Immunology, Medical University of South Carolina, 173 Ashley Avenue, Charleston, SC 29425, USA

⁵Department of Microbiology and Molecular Genetics, Medical College of Wisconsin, 8701 Watertown Plank Road, Milwaukee, WI 53226, USA

⁶Department of Biochemistry and Molecular Biology, Medical University of South Carolina, 173 Ashley Avenue, Charleston, SC 29425, USA

⁷Hollings Cancer Center, Medical University of South Carolina, 86 Jonathan Lucas Street, MSC 955, Charleston, SC 29425, USA

⁸Department of Medicine and Penn Institute for Regenerative Medicine, Perelman School of Medicine, University of Pennsylvania, Philadelphia, PA 19104, USA

⁹Papé Family Pediatric Research Institute, Oregon Health & Science University, 3181 South West Sam Jackson Park Road/L321, Portland, OR 97239, USA

¹⁰Lead Contact

*Correspondence: duncanst@musc.edu

<http://dx.doi.org/10.1016/j.stem.2017.01.011>

SUMMARY

Efforts to identify pharmaceuticals to treat heritable metabolic liver diseases have been hampered by the lack of models. However, cells with hepatocyte characteristics can be produced from induced pluripotent stem cells (iPSCs). Here, we have used hepatocyte-like cells generated from homozygous familial hypercholesterolemia (hoFH) iPSCs to identify drugs that can potentially be repurposed to lower serum LDL-C. We found that cardiac glycosides reduce the production of apolipoprotein B (apoB) from human hepatocytes in culture and the serum of avatar mice harboring humanized livers. The drugs act by increasing the turnover of apoB protein. Analyses of patient medical records revealed that the treatment of patients with cardiac glycosides reduced serum LDL-C levels. These studies highlight the effectiveness of using iPSCs to screen for potential treatments for inborn errors of hepatic metabolism and suggest that cardiac glycosides could provide an approach for reducing hepatocyte production of apoB and treating hypercholesterolemia.

INTRODUCTION

The Next Generation Genetic Association Studies consortium was developed to provide a functional dimension to the genomic

study of cardiovascular disease. The primary goal of this initiative is to exploit the power of cellular reprogramming to generate induced pluripotent stem cells (iPSCs) from thousands of patients with defined genetic variations that correlate with cardiovascular disease. To date, iPSC lines produced by the consortium are available from genotyped patients with coronary artery disease, platelet aggregation deficiencies, lipid disorders, QT interval and ECG cardiac traits, pulmonary hypertension, insulin resistance, left ventricular hypertrophy, myocardial infarction, and sickle cell anemia (<http://www.wicell.org/home/stem-cell-lines/collections/collections.cmsx>). Having banks of patient-specific iPSCs provide investigators with cells for functional studies and drug discovery. As proof of feasibility we, therefore, sought to use iPSC-derived hepatocyte-like cells (referred to here as hepatocytes) from a familial hypercholesterolemia patient for a screen to identify pharmaceuticals that could be used to treat hypercholesterolemia in a low-density lipoprotein receptor (LDLR)-independent manner.

Familial hypercholesterolemia is a disease caused primarily by mutations in the LDLR. The disease is characterized by elevated serum LDL-cholesterol (LDL-C). In patients with compound heterozygous or homozygous mutations in the LDLR (referred to collectively as hoFH), LDL-C levels reach >500 mg/dL, which lead to the formation of xanthomas, severe cardiovascular disease, and early death (Rader et al., 2003). Importantly, although the LDLR is broadly expressed, the disease can be cured by liver transplantation, indicating that the hepatic LDLR is the primary regulator of serum LDL-C levels (Alphonse and Jones, 2016). Most drugs that lower serum LDL-C work on the liver through up-regulation of *LDLR* transcription (statins) or stability of the LDLR protein (proprotein convertase subtilisin/kexin type 9 [PCSK9]

inhibitors) (Nissen et al., 2016; Thompson et al., 2003). As a consequence, such drugs are relatively ineffective in patients with hoFH (Cuchel et al., 2014). However, therapies that limit hepatic production of VLDL, the precursor to LDL, are effective in reducing LDL-C in patients with hoFH (Rader and Kastelein, 2014; Davidson, 2009). Lomitapide inhibits the microsomal triglyceride transfer protein (MTP), which is critical for hepatic VLDL assembly and reduces LDL-C by approximately 40%–50%. Mipomersen is an antisense oligonucleotide that targets the mRNA encoding apoB, the essential core protein of VLDL, in the liver and reduces LDL-C by approximately 25% in hoFH patients. Both of these drugs reduce hepatic secretion of VLDL and apoB independently of the LDLR, but unfortunately result in increased fat in the liver (Rader and Kastelein, 2014).

To demonstrate the utility of using iPSC-derived hepatocytes as a platform to identify drugs that could be used to treat metabolic liver disease, we used hoFH iPSC-derived hepatocyte-like cells for a screen of a library of existing drugs that could potentially be repurposed (Strittmatter, 2014). Drugs that reduce apoB levels in the media of hoFH hepatocytes should act independently of the LDLR and so we reasoned that success could provide an alternative treatment for hoFH and other forms of difficult-to-treat hypercholesterolemia.

RESULTS

Small Molecule Screen using hoFH iPSC-Derived Hepatocyte-like Cells

Success in identifying drugs that can be used to target a rare disease relies on the development of screening assays. Unfortunately, primary hepatocytes rapidly de-differentiate upon culture and given the variability in the genetics of the donors pose challenges for use in high throughput drug discovery (Binda et al., 2003). Recently, technologies have been developed to produce iPSCs from patients (Takahashi et al., 2007; Yu et al., 2007). Since patient-specific iPSCs can be induced to differentiate into a variety of cell types, including cells with hepatocyte characteristics, investigators can now model heritable human diseases in culture and screen for therapeutics (Lee et al., 2009; Ebert et al., 2009; Rashid et al., 2010; Matsu et al., 2014; Robinson and Daley, 2012; Choi et al., 2013; Szkolnicka et al., 2016; Cameron et al., 2015; Lang et al., 2016; Schwartz et al., 2012; Mallanna et al., 2016). We have previously described the generation of iPSCs from a hoFH patient (Cayo et al., 2012). The patient has a deletion in exon 17 of the maternal allele, which is a null mutation, and an A-G transition in exon 17 of the paternal allele, which encodes a receptor that is unable to internalize LDL (Davis et al., 1986). When hepatocyte-like cells are generated from these hoFH iPSCs, they faithfully recapitulate the pathophysiology associated with the liver of hoFH patients (Cayo et al., 2012). In these experiments, hoFH hepatocytes failed to traffic exogenous LDL to endosomes and were unable to increase LDL clearance in response to statin treatment. Moreover, compared to controls, the hoFH iPSC-derived hepatocytes had elevated levels of apoB in the culture medium (Cayo et al., 2012).

The high level of apoB in the medium of hoFH iPSC-derived hepatocytes potentially offers a screenable phenotype for identification of new LDL-C lowering drugs. Any drug capable of reducing LDL-C in the medium of hoFH iPSC-derived hepat-

cytes must act through a mechanism that is independent of the LDLR. We, therefore, measured apoB in the media by ELISA as our primary assay. A comparison of the ELISA performance on positive and negative control cells confirmed that the assay was appropriate for screening (Z -factor = 0.88) (Figure 1A). Moreover, the ELISA could distinguish the effect of treating iPSC-derived hepatocytes with vehicle or the protein synthesis inhibitor cycloheximide as a positive control ($p = 9.7 \times 10^{-28}$) (Figure 1B). We have previously described the production of hepatocyte-like cells from iPSCs using monolayer culture and completely defined conditions (Si-Tayeb et al., 2010a; Mallanna and Duncan, 2013). The procedure is efficient with approximately 80% of cells expressing hepatocyte markers and is highly reproducible with minimal well-to-well variation (Figure 1A). The hoFH iPSCs were differentiated into hepatocyte-like cells in 96-well plates and the levels of apoB measured before and after the application of 2,320 small molecules from the Spectrum collection drug library (Figure 1C). The library was selected because it contains ~1,300 drugs that have reached clinical trials in the USA, Europe, or Japan. Also, the library has ~800 compounds that are natural products. Compounds in the library are structurally diverse and include oxygen heterocycles, diterpenes, sesquiterpenes, pentacyclic triterpenes, and alkaloids. Moreover, the library has been previously used to identify drugs for repurposing (Weisman et al., 2006; Kocisko et al., 2003; Fagan et al., 2013; Wang et al., 2010).

The pre- to post-drug treatment ratio of apoB was established for each compound (Figure 1D) and hits identified by Z score analysis (Figure 1E) as described by Zhang (2011). Ratios that had a z score of ≤ -3 (decreased apoB) or ≥ 3 (increased apoB), based on the 3-sigma rule, were considered primary hits. Using these criteria, we found eight drugs that increased and 21 that decreased apoB levels in the culture medium (Table S1). Next, the effect of each drug on apoB levels was compared to vehicle (DMSO) controls ($n = 3$ biological replicates). Of the 29 drugs identified in the initial screen, 55% were reproducible ($p \leq 0.05$), with 13 compounds decreasing the level of apoB (Figure 2A). Of the compounds that reproducibly decreased apoB secretion, five were cardiac glycosides, sharing a similar molecular structure (Figure 2B). If we reduced the stringency of the z score to ≤ -2.0 in the primary screen, 7 of 9 cardiac glycosides present in the library were identified (Figure 2C). We, therefore, tested all nine of the cardiac glycosides in the Spectrum collection in triplicate assays to determine whether they all reduced levels of apoB in the medium of iPSC-derived hepatocytes (Figure 2A). Remarkably, every cardiac glycoside tested reduced apoB compared to pre-treatment levels and DMSO-treated controls ($p \leq 0.05$). Reductions ranged from 29% (ouabain) to 73% (gitoxin) (Figure 2C).

We predicted that the ability of cardiac glycosides to lower apoB should not be restricted to hoFH cells. To determine whether the cardiac glycosides also reduced apoB levels in wild-type hepatocytes, we established dose-response curves using HepG2 hepatoma cells (Figure 3A), primary human hepatocytes (Figure 3B), and hepatocyte-like cells derived from control (K3) iPSCs (Figure S1) (Si-Tayeb et al., 2010b). With the exception of strophanthidin, which was less efficient, the cardiac glycosides reduced apoB levels with an $EC_{50} \leq 20$ nM. Based on these data, we conclude that cardiac glycosides have an unappreciated

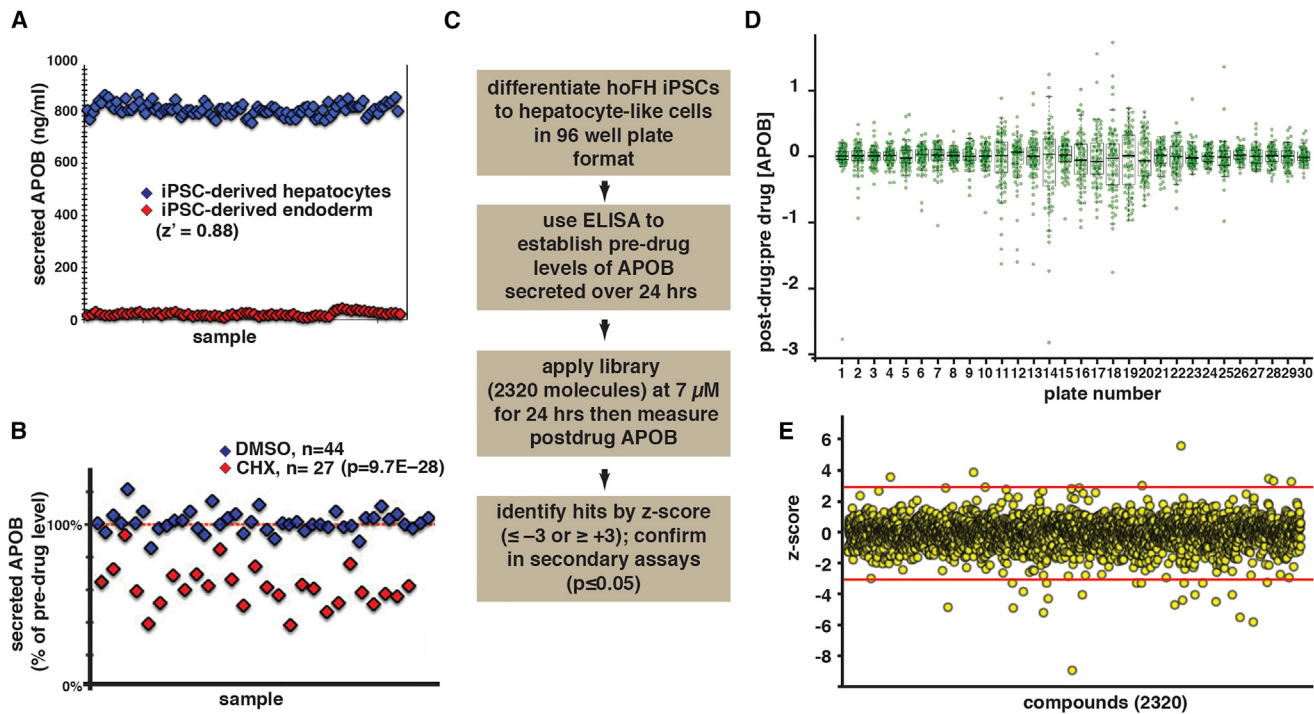


Figure 1. A Screen for Small Molecules that Reduce apoB Production from hoFH iPSC-Derived Hepatocyte-like Cells

(A) Graph revealing that an ELISA can efficiently and reliably ($z' = 0.88$) distinguish between cells that do (iPSC-derived hepatocytes, blue) and do not (iPSC-derived endoderm, red) secrete apoB.

(B) ELISA can also distinguish between the levels of apoB in the medium of iPSC-derived hepatocytes treated with either vehicle (DMSO, blue) or the protein synthesis inhibitor cycloheximide (CHX, red).

(C) Schematic overview of the protocol used to identify small molecules that reduce apoB production from hoFH iPSC-derived hepatocyte-like cells.

(D) Graph showing the post-drug:pre-drug ratios of apoB identified in the culture medium from the primary screen. The green circles represent individual drugs within the library, and the box and whisker plots summarize the mean and distributions for each plate (30 plates).

(E) Graph showing z scores (red lines = ± 3) of the effect of 2,320 drugs (yellow spheres) on the concentration apoB in the culture medium of treated cells.

ability to lower the levels of apoB in culture medium from both LDLR-deficient and wild-type hepatocytes.

Cardiac Glycosides Enhance Proteolytic Turnover of apoB Protein

We sought to address the mechanism through which the cardiac glycosides reduced the concentration of apoB in the medium. Since apoB is the central protein component of VLDL and LDL particles, we first determined whether cardiac glycoside treatment resulted in a reduction in VLDL/LDL. Lipoprotein production was measured by [3 H]-glycerol labeling of triglycerides followed by FPLC in primary human hepatocytes treated with either DMSO, digoxin, or proscillarin (Figure 4A). As expected, both digoxin and proscillarin dramatically reduced VLDL triglyceride levels in the medium of glycoside treated hepatocytes. We next examined the kinetics of apoB accumulation in the culture medium of hoFH iPSC-derived hepatocytes in the presence and absence of digoxin, proscillarin, or convallatoxin over time. As shown in Figure 4B, hoFH cells treated with each of the glycosides exhibited a reduction in the concentration of apoB in the medium compared to DMSO within 60 min of treatment. This rapid response to glycoside administration implied that the effect of the drug was direct rather than an indirect change in cell behavior. Based on this implication, we reasoned that the drug

could influence either expression of the *APOB* gene, apoB protein synthesis, post-translational control of apoB protein, or secretion. Steady-state mRNA levels encoding apoB were determined in wild-type (K3) iPSC-derived hepatocytes by qRT-PCR and found to be unaffected by treatment with either digoxin or proscillarin (Figure 4C). We next determined whether synthesis of apoB protein was affected by metabolic labeling of nascent proteins followed by immunoprecipitation in the presence or absence of digoxin (Figure 4D). We first confirmed the specificity of antibodies used to precipitate apoB. As expected, proteins were not precipitated by anti-apoB antibody from lysates of undifferentiated iPSCs that do not express apoB. Similarly, protein was undetected when lysates from iPSC-derived hepatocytes were subjected to precipitation using an anti-FLAG control antibody. When precipitations of apoB were performed on lysates from iPSC-derived hepatocytes labeled with [35 S]-Methionine, nascent apoB protein levels were indistinguishable between untreated- and digoxin-treated cells despite the fact that digoxin reduced the level of apoB in the cell medium. Based on these studies, we conclude that cardiac glycosides have no effect on expression of *APOB* or the synthesis of apoB protein and that these drugs must act post-translationally.

Post-translational control of apoB-100 protein has been studied in detail and has been shown to be highly regulated

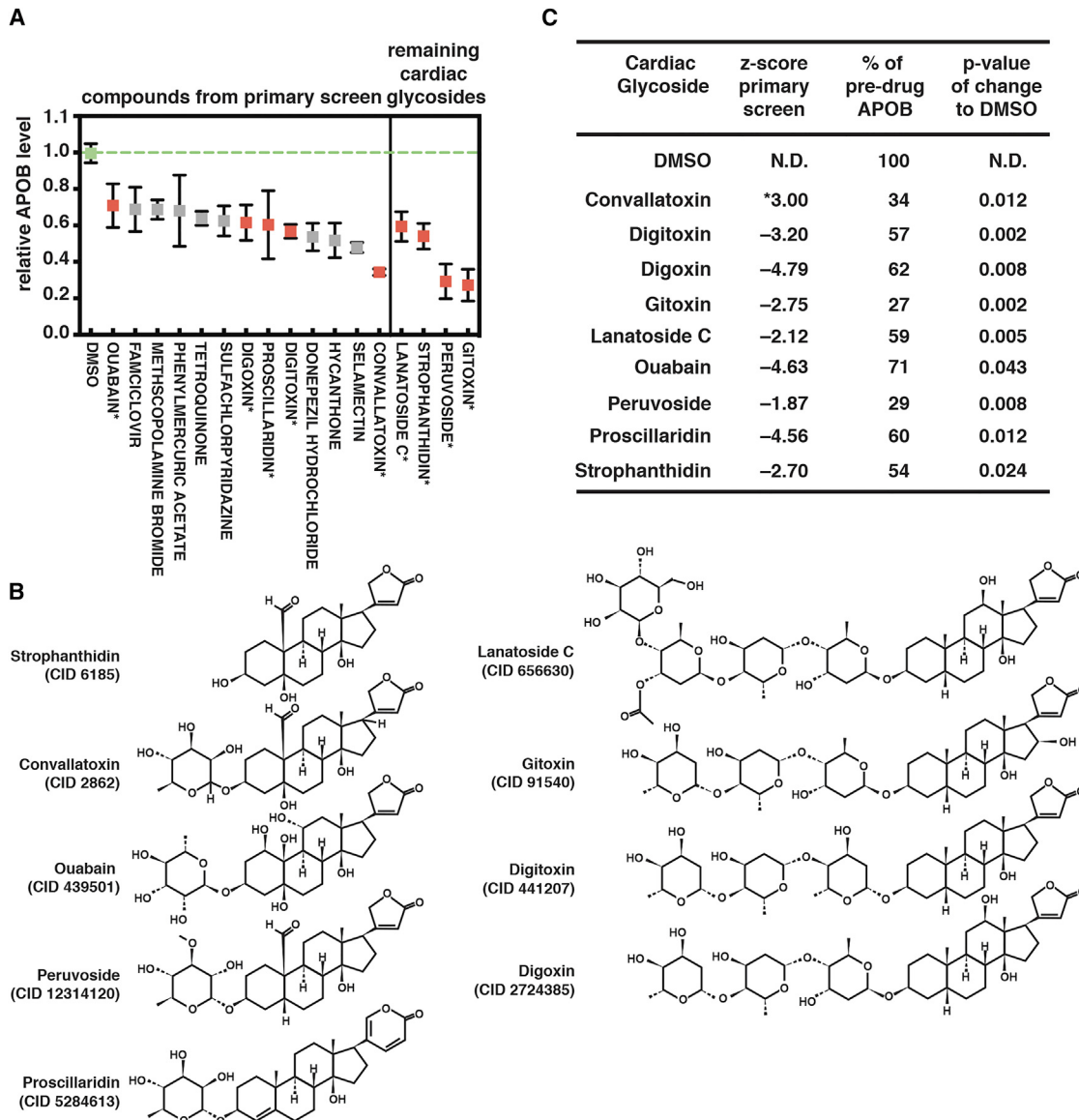


Figure 2. Cardiac Glycosides Inhibit the Concentration of apoB in the Medium of Cultured Hepatic Cells

(A) Box and whisker plot demonstrating that 13 small molecules, including five cardiac glycosides (red, asterisks) that were identified as hits in the primary screen, plus four additional cardiac glycosides (red, asterisks) present in the library, reproducibly ($n = 3$, $p \leq 0.05$) inhibit the levels of apoB measured in the culture medium compared to iPSC-derived hepatocytes treated with vehicle (DMSO, dashed line).

(B) Structure of cardiac glycosides present in the library that were found to inhibit apoB production.

(C) Table showing the quantitative effect of cardiac glycosides on the levels of apoB secreted by hoFH iPSC-derived hepatocyte-like cells.

and crucial for the formation and secretion of lipoprotein particles (Ginsberg and Fisher, 2009; Sundaram and Yao, 2010). We, therefore, examined the steady-state intracellular levels of apoB protein by immunoblot analyses of iPSC-derived hepatocytes treated for 24 hr with either DMSO, the protein synthesis inhibitor cycloheximide as a control for protein turnover, digoxin, or proscillaridin. As expected, compared to DMSO-treated control cells, cycloheximide resulted in an 8-fold reduction in the cellular level of apoB protein as the intracellular pool of apoB was degraded or secreted (Figure 4E). Strikingly, treatment of the cells with either digoxin or proscillaridin resulted in a similar

reduction in the level of intracellular apoB (Figure 4E). When cells were treated with both cycloheximide and a cardiac glycoside, the reduction in apoB protein level was exacerbated. Using ELISA, we confirmed that digoxin and proscillaridin reduced the level of apoB ($p < 0.05$, $n = 3$ biological replicates) in the media of samples used for immunoblot and qRT-PCR analyses (Figure 4F).

The observation that intracellular apoB levels were reduced even though synthesis of apoB protein was unaffected by cardiac glycoside treatment implied that the glycosides act by promoting apoB degradation. Degradation of newly synthesized

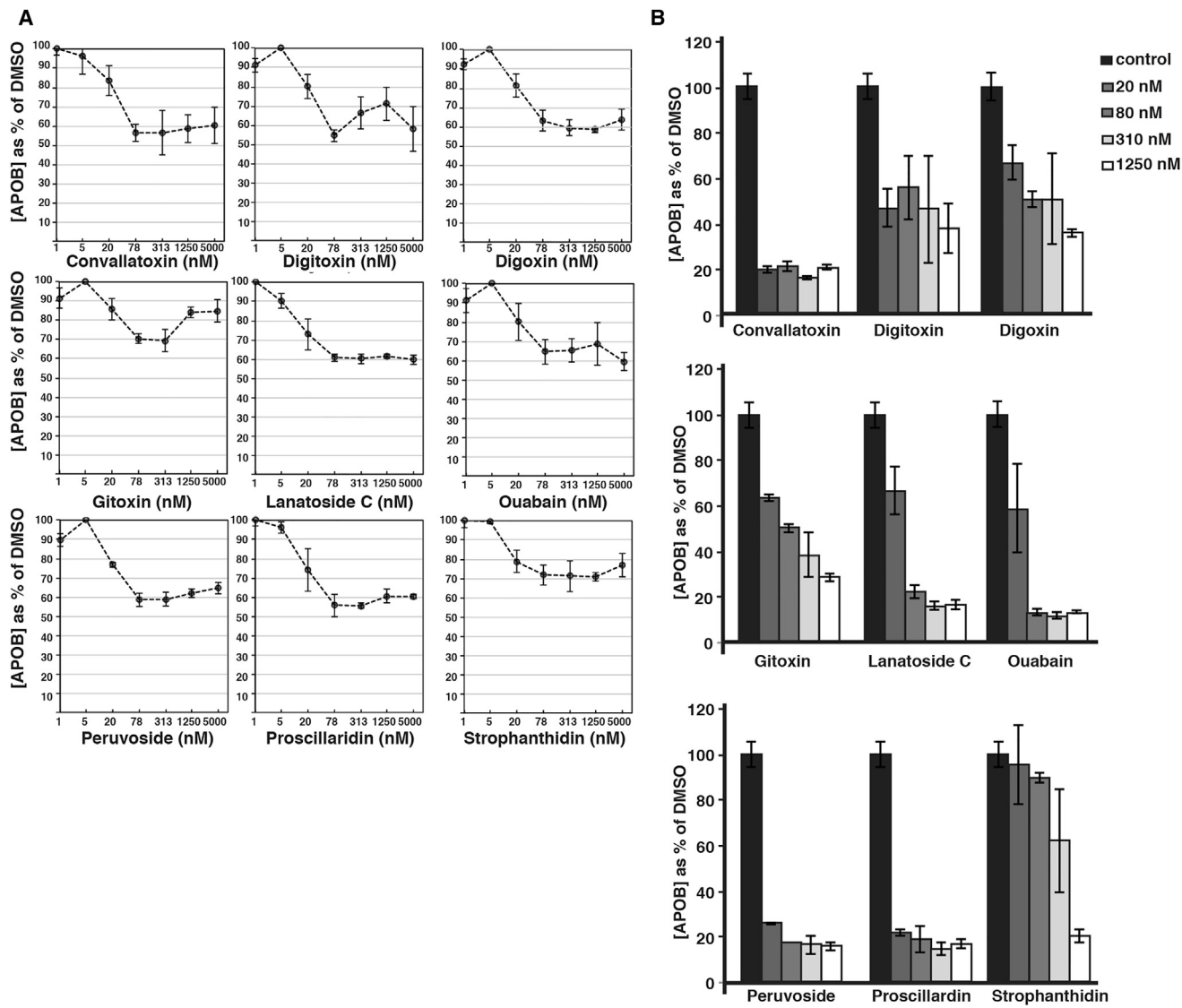


Figure 3. Cardiac Glycosides Inhibit apoB Production at Nanomolar Concentrations

(A and B) Graphs showing 8-point dose response curves generated from the treatment of HepG2 cells (A) or primary human hepatocytes with various cardiac glycosides (B) at 1; 5; 20; 78; 312; 1,250; and 5,000 nM. See Figure S1 for dose response performed on iPSC-derived hepatocytes.

apoB occurs predominantly by the proteasome and regulates lipoprotein production (Fisher and Ginsberg, 2002; Liang et al., 1998). We, therefore, addressed whether glycoside-mediated reduction in apoB levels could be rescued by pharmacological inhibition of proteasome activity. Hepatocytes were produced from wild-type iPSCs and treated for 8 hr with either DMSO, digoxin, or digoxin plus the proteasome inhibitor MG132 before measuring apoB by immunoblot (Figure 4G). Although we observed variation between different experiments, in all cases (Figure 4H; $n = 4$ biological replicates), we found that the addition of MG132 to digoxin-treated hepatocytes increased the level of intracellular apoB. From these data, we conclude that the cardiac glycosides enhance the turnover of apoB at least in part through promoting proteasome-mediated degradation.

LDL-C Levels Are Reduced in Human Patients Treated with Cardiac Glycosides

Cardiac glycosides are used to treat congestive heart failure and atrial fibrillation (Hothi et al., 2013; Ambrosy et al., 2014). Although the use of cardiac glycosides has declined, at its peak, digoxin was used to treat 80% of patients with heart failure (Hothi et al., 2013). Despite the clinical use of cardiac glycosides for over 200 years, their ability to reduce human LDL-C levels has not been reported. We, therefore, examined whether cardiac glycosides had LDL-C lowering properties in humans by examining the medical records of patients who had entered the Froedtert Hospital/Medical College of Wisconsin clinics. We first identified a cohort of patients who had historically been prescribed with a cardiac glycoside ($n = 5,493$). Within this group, we also identified patients who had been prescribed an

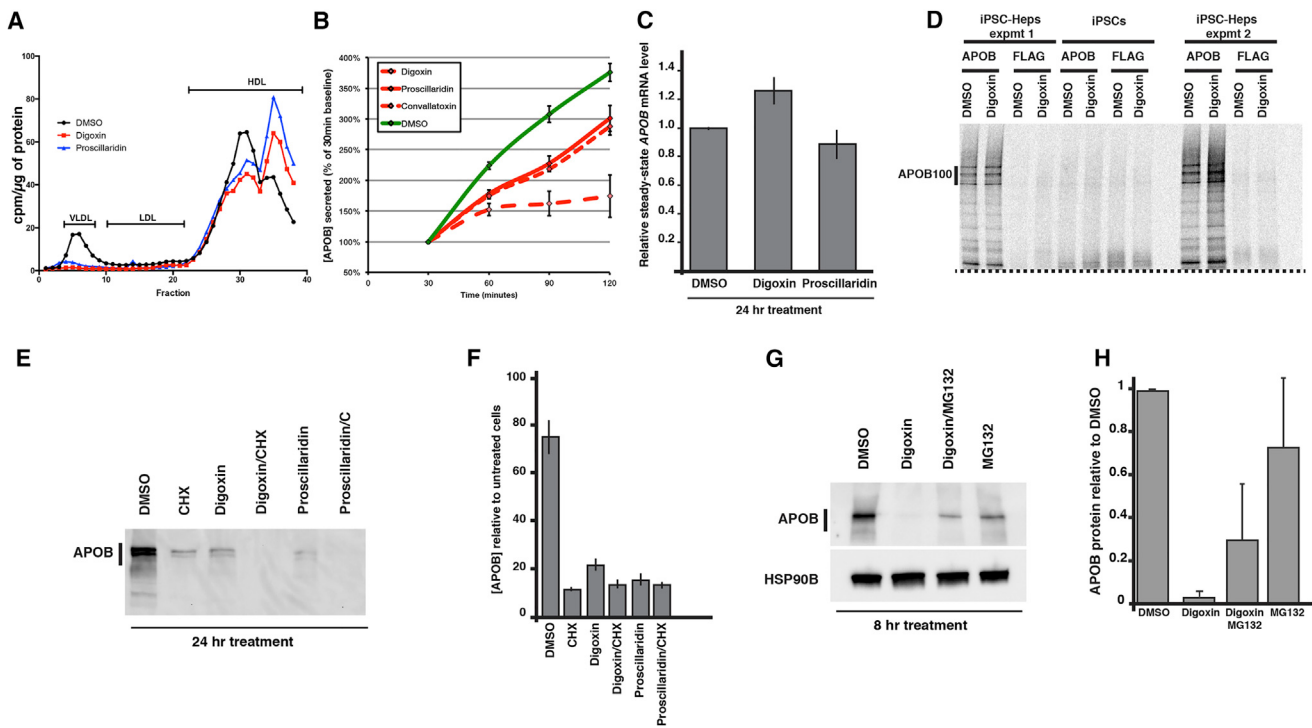


Figure 4. Cardiac Glycosides Reduce Steady-State Cellular Levels of apoB Protein

(A) Graph showing the effect of 16 hr treatment with digoxin (310 nM) and proscillaridin (310 nM) compared to DMSO (vehicle) on the production of lipoprotein particles by primary human hepatocytes. The lipoproteins were identified after labeling triglycerides with [³H]-glycerol and separation by FPLC.

(B) Graph showing the effect of digoxin, proscillaridin, and convallatoxin (50 nM) compared to DMSO on the level of apoB in the medium of iPSC-derived hepatocytes ($n = 4$ biological replicates) over 2 hr of treatment.

(C) Bar graph showing the quantification of apoB mRNA by RT-qPCR in iPSC-derived hepatocytes treated with DMSO, digoxin, or proscillaridin ($n = 4$ biological replicates).

(D) Micrograph showing results of metabolic labeling analyses of apoB. There were two sets of iPSC-derived hepatocytes (iPSC-Heps expmt 1 and 2) and undifferentiated iPSCs that were labeled for 30 min with [³⁵S]-Met in the presence of DMSO or digoxin (310 nM). The lysates were subjected to immunoprecipitation using anti-apoB (apoB) and anti-FLAG antibodies. The dashed line indicates the bottom portion of gel that was digitally masked using Adobe Illustrator.

(E) Micrograph showing example of immunoblot analysis of iPSC-derived hepatocytes treated for 24 hr with DMSO, cycloheximide (CHX, 100 μ M), digoxin (310 nM), and/or proscillaridin (310 nM).

(F) Bar graph showing ELISA quantification of apoB in the medium of iPSC-derived hepatocytes treated for 24 hr with DMSO, cycloheximide (CHX, 100 μ M), digoxin (310 nM), and/or proscillaridin (310 nM).

(G) Immunoblot measuring the level of apoB after treating the cells for 8 hr with DMSO, digoxin (310 nM), digoxin (310 nM) + MG132 (10 μ M), or MG132 (10 μ M) alone.

(H) Quantification of biological replicates ($n = 4$) of immunoblots on samples treated as in (G).

angiotensin-converting-enzyme (ACE) inhibitor, which should have no effect on cholesterol levels, or a statin, which served as a positive control group. Since the time frame during which a patient was prescribed a particular medication was known, it was possible to retrieve serum LDL-C and serum albumin measurements that had been recorded when patients were either “on” or “off” of drug treatment (Figure 5). Patients prescribed with each drug were therefore split into cohorts depending on whether they were on or off of drug when their LDL-C or albumin was measured. An ACE-inhibitor had no significant impact on the serum levels of either LDL-C (off drug $n = 165$ and on drug $n = 180$, $p = 0.44$) or albumin (off drug $n = 763$ and on drug $n = 1,767$, $p = 0.24$) (Figures 5A and 5B). As expected, treatment with a statin was associated with a reduction in the mean serum LDL-C from 103.6 ± 2.2 mg/dL in off drug patients to 89.8 ± 1.9 mg/dL in on drug patients (off drug $n = 204$ and on drug $n = 221$, $p < 0.0001$), while albumin levels were unaffected (off

drug $n = 906$ and on drug $n = 1,865$) (Figures 5A and 5B). Strikingly, patients prescribed a cardiac glycoside displayed a reduction in serum LDL-C levels that was similar to patients treated with a statin, 103.1 ± 1.8 mg/dL in off drug to 94.0 ± 2.3 mg/dL in on drug patients (off drug $n = 205$ and on drug $n = 324$, $p = 0.0019$), with no effect on serum albumin (off drug $n = 2,116$ and on drug $n = 770$) (Figures 5A and 5B).

The above analysis relied on cohorts of patients in which LDL-C measurements were taken either inside (on drug) or outside (off drug) the window of an active prescription. However, the LDL-C measurements of on drug and off drug cohorts were not necessarily from the same patients. We recognized that definitive human data would require us to retrieve on drug and off drug LDL-C measurements that could be matched to individuals. This would allow us to determine whether serum LDL-C dropped after a specific patient was given a cardiac glycoside. In searching medical records, we identified patients who had

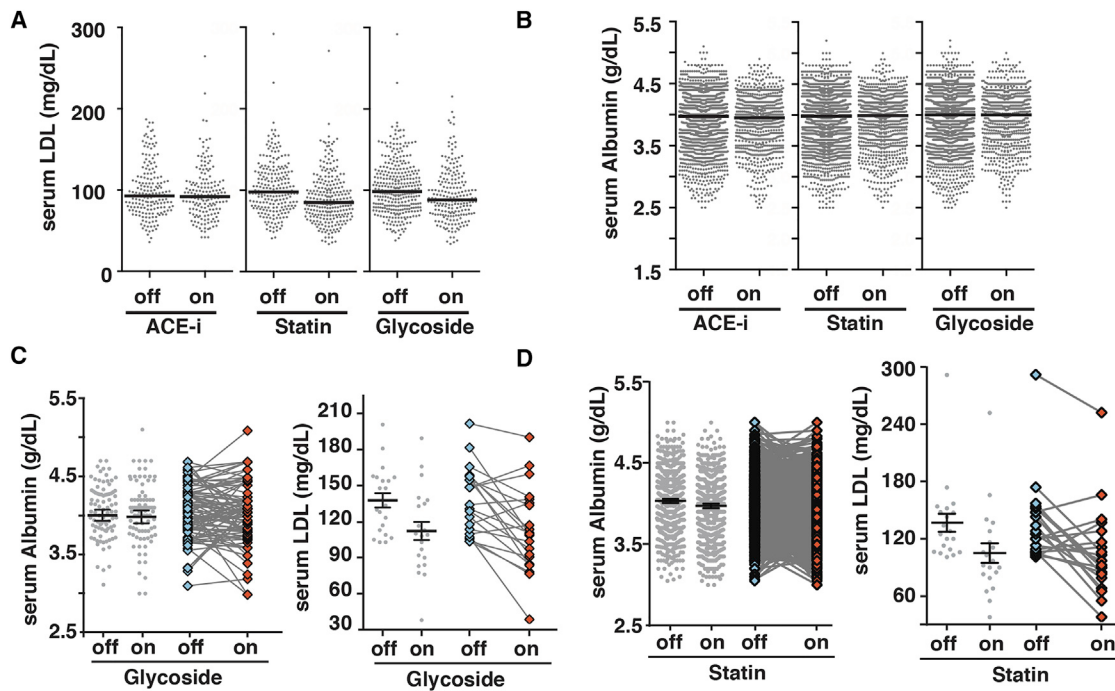


Figure 5. Human Patients Treated with Cardiac Glycosides Have Reduced Serum LDL-C Levels

(A) Graph showing concentration of LDL in the serum of a cohort of patients (gray circles) when on or off treatment with an ACE inhibitor (ACE-i) (on n = 180 and off n = 165), a statin (on n = 221 and off n = 204), or a cardiac glycoside (on n = 324 and off n = 205). The black bar shows the mean LDL concentration.

(B) Graphs showing the concentration of albumin in the serum of patients (gray circles) when on or off treatment with the indicated drugs. ACE inhibitor (ACE-i) (on n = 1,767 and off n = 763), a statin (on n = 1,865 and off n = 906), or a cardiac glycoside (on n = 2,116 and off n = 770) are shown. The black bar shows the mean albumin concentration.

(C) Graphs showing serum albumin (left, n = 87) and LDL (right, n = 21) measurements in the same patients before and after treatment with cardiac glycosides. The black bar shows the mean concentration, and the gray lines indicate the direction of change in each patient when off (blue diamonds) or on (red diamonds) the medication.

(D) Graphs showing serum albumin (left, n = 715) and LDL-C (right, n = 91) measurements in the same patients before and after treatment with statins. The black bar shows the mean concentration, and the gray lines indicate the direction of change in each patient when off (blue diamonds) or on (red diamonds) the medication.

measurements of albumin (n = 91) or LDL-C (n = 21) taken both within and outside of treatment with a cardiac glycoside (Figure 5C). A similar cohort of patients treated with a statin was again used as a positive control (Figure 5D). The serum levels of albumin in these patients were once more unaffected by drug treatment. In contrast, patients displayed a mean serum LDL-C reduction of 31.8 ± 8.6 mg/dL ($p = 0.0016$) during treatment with statins and 25.6 ± 6.3 mg/dL ($p = 0.0006$) with cardiac glycosides. In 16 of the 21 patients examined, LDL-C levels had dropped substantially following the administration of a cardiac glycoside (Figure 5C).

Cardiac Glycosides Reduce LDL-Cholesterol Levels in Humanized Avatar Mice

Although these retrospective analyses of electronic medical records were convincing, we acknowledged that in contrast to a clinical trial, interpretation of results could be confounded by random variables such as diet, adherence, other drug use, physical condition, etc. We reasoned that it was important to test directly the in vivo effect of the cardiac glycosides in human hepatocytes under controlled conditions. We, therefore, generated avatar mice (Figures 6A and S2) in which human hepatocytes

replaced the endogenous murine hepatocytes (Azuma et al., 2007; Wilson et al., 2014). Importantly, mice harboring humanized livers have previously been shown to adopt a typical human lipoprotein profile (Ellis et al., 2013; Bissig-Choisat et al., 2015). Such animals, therefore, provide an ideal model in which to test the cholesterol-lowering properties of cardiac glycosides on human hepatocytes *in vivo*.

Avatars were produced using hepatocytes from two donors. Donor A was a 53-year-old female and donor B was a 17-year-old male. We measured serum apoB and albumin levels by ELISA using human-specific antibodies (Figures S2 and S3) after treatment with DMSO (vehicle), digoxin, or proscillaridin. Based on our study of the action of cardiac glycosides on iPSC-derived hepatocytes, we expected the response to glycoside treatment to be rapid, and so we measured the serum levels of apoB after providing three intraperitoneal injections of glycosides over a 48 hr period. We selected a dose that was 1/8 of the reported LD₅₀ for each drug, which equated to 0.5 mg/kg/day for digoxin and 0.6 mg/kg/day for proscillaridin and was within the published range (from 0.1 mg to 2 mg/kg/day). We did not know the relative level of LDL-C of the original hepatocyte donors, however, the ratio of apoB to albumin was approximately 30%

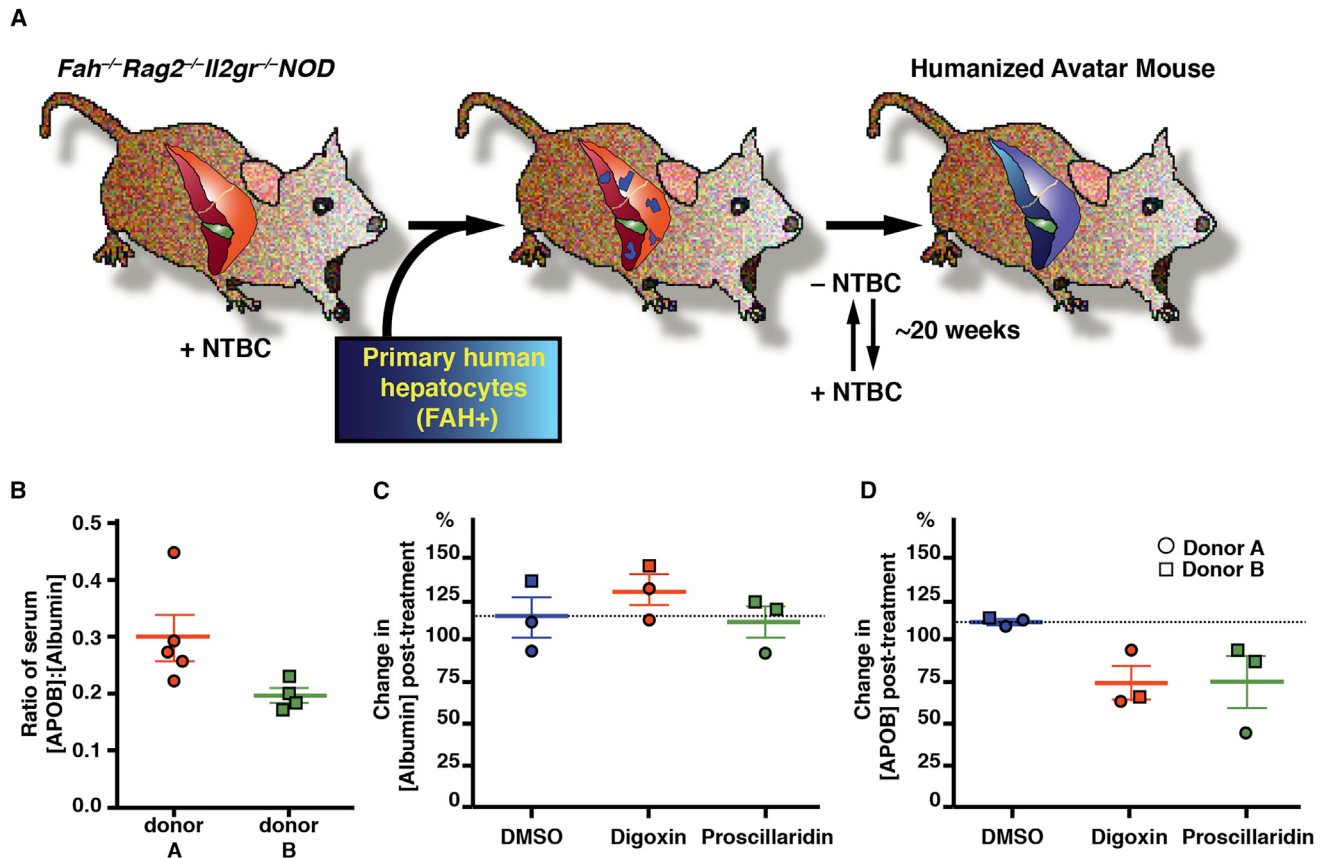


Figure 6. Cardiac Glycosides Reduce Serum Levels of Human apoB in Humanized Mice

(A) Illustrated overview of the procedure for the generation of *Fah^{-/-}Rag2^{-/-}Ii2gr^{-/-}NOD* mice harboring human hepatocytes.

(B) Graph showing the ratio of human albumin to human apoB found in the serum of avatar mice harboring hepatocytes from two different donors (donor A red circles and donor B green squares) ($n = 9$).

(C) Graph showing that treatment of avatar mice (donor A circles and donor B squares) with vehicle (DMSO, blue), digoxin (red), or proscillarinidin (blue) had no effect on albumin levels.

(D) Graph showing the percent change in the concentration of apoB found in the serum of avatar mice (donor A circles and donor B squares) treated with vehicle (DMSO, blue), digoxin (red), or proscillarinidin (blue). See Figure S2 for characterization of FRGN mice and antibodies. See Figure S3 for data on individual mice.

higher in the serum of avatars repopulated with hepatocytes from donor A compared to donor B (Figure 6B). Importantly, the levels of human albumin in the serum were unaffected by treatment with digoxin or proscillarinidin (Figure 6C). However, in contrast to DMSO, which had no effect, treatment of the avatar mice with either of the cardiac glycosides significantly reduced serum apoB levels ($p \leq 0.05$, $n = 3$ biological replicates) regardless of donor (Figures 6D and S3).

DISCUSSION

We have used hepatocyte-like cells derived from hoFH iPSCs in a screen to identify drugs that could potentially be used to treat hypercholesterolemia. Because the hoFH hepatocytes lack a functional LDLR receptor, the effective compounds should act on pathways that are independent of the LDLR. In addition to their potential utility in hoFH patients, such drugs could be useful for lowering LDL-C in patients that cannot reduce their LDL-C sufficiently using existing therapies.

The identification of novel pharmaceuticals, especially for rare diseases, has historically been hampered by the limited availability of cell models that accurately reflect the pathophysiology of the disease (Horvath et al., 2016). Most commonly, cell-based assays have relied heavily on immortalized or cancer cell lines. However, long term culture of such cells results in genetic drift where the cells accumulate genetic rearrangements, aberrant chromosomal copy numbers, and disrupted epigenetic states. Despite these disadvantages, hepatoma cells have been used to identify small molecules with potential therapeutic application. Relevant to the current work, HepG2 cells were recently used to identify small molecules that can increase expression of Tribbles Pseudokinase 1 (TRIB1) (Nagiec et al., 2015). This finding was provocative because genome wide association studies have linked TRIB1 to cardiovascular disease, and overexpression of TRIB1 can inhibit secretion of VLDL (Nagiec et al., 2015). Primary cells could potentially circumvent problems associated with genetic drift, however, because each preparation of primary hepatocytes comes from a unique donor, genetic variability among

donors can significantly impact the reproducibility of screening efforts. Moreover, using primary hepatocytes to model metabolic dysfunctions can be problematic because it is logistically challenging to obtain primary cells from patients with rare diseases. Induced pluripotent stem cells could offer an alternative and robust cell platform for drug discovery (Matsa et al., 2014; Kimbrel and Lanza, 2015). Human iPSCs retain a relatively stable genomic environment, provide an indefatigable source of cells, can be genetically manipulated, and procedures for producing patient-specific iPSCs are relatively straightforward. A large number of protocols have been described that facilitate the production of hepatocyte-like cells from pluripotent stem cells (Cai et al., 2007; Hay et al., 2008; Basma et al., 2009; Song et al., 2009; Touboul et al., 2010; Sullivan et al., 2010; Si-Tayeb et al., 2010a; Asgari et al., 2011). Despite the large number of procedures, in most, if not all, differentiation conditions, iPSC-derived hepatocytes do not recapitulate the full repertoire of liver functions. This caveat is important with regard to drug discovery because a failure to generate fully functional hepatocytes can influence first pass metabolism, can impact drug toxicity profiles (Berger et al., 2015), and, in some cases, may prevent the cells from accurately modeling the target disease (Davidson et al., 2015).

Despite caveats, several laboratories have reported the successful generation of iPSCs from patients with a variety of inborn errors of hepatic metabolism and have demonstrated that hepatocytes derived from them can recapitulate the pathophysiology of the disease in culture (Rashid et al., 2010; Cayo et al., 2012; Choi et al., 2013; Tafaleng et al., 2015; Leung et al., 2013; Yi et al., 2012; Li et al., 2015; Zhang et al., 2011). Although the generation of models of hepatic disease using iPSCs has been successful, very few have been translated into platforms for drug screening. Choi and colleagues used iPSCs from a patient with alpha-1 antitrypsin (AAT) deficiency to screen 3,131 molecules from The Johns Hopkins' Drug Library and found five existing drugs that had a capacity to reduce accumulation of misfolded alpha-1 antitrypsin (Choi et al., 2013). In a small-scale screen of five autophagy-inducing drugs, Maetzel and colleagues demonstrated improved autophagic response in hepatocytes generated from Niemann-Pick type C (NPC) iPSCs (Maetzel et al., 2014). Part of the challenge of using iPSC-derived hepatocytes in a drug screening project lies in ensuring that the quality of the differentiations is reproducible, synchronous, and efficient. Our use of a relative simple differentiation protocol that relies on cell monolayers and completely defined culture conditions is highly compatible with high throughput analyses. In addition, with the advent of genomic engineering, targeted generation of mutations using CRISPR-CAS 9 within iPSCs is relatively simple (Ding et al., 2013). Exploiting the power of genomic engineering, therefore, obviates any requirement to access a patient population and so even the rarest of rare diseases can be potentially modeled. This capability is important because it makes the discovery of drugs to treat rare disorders accessible to an academic laboratory.

To the best of our knowledge, there has been no account of a direct effect of cardiac glycosides on lowering LDL-C in humans. However, extract of *Nerium oleander*, which contains glycosides and polyphenols, has been shown to reduce plasma lipoprotein concentrations in a rat model of induced hyperlipidemia (Gaya-

thri et al., 2011). Studies using cardiac glycosides have also previously been performed on HepG2 hepatoma cells (Campia et al., 2009; Kolkhof et al., 2010). In one study, treatment of HepG2 cells with either digoxin or ouabain increased intracellular cholesterol synthesis by enhancing expression and activity of HMG-CoA reductase through the SREBP2/SCAP complex (Campia et al., 2009). However, when we measured the amount of apoB in the medium of HepG2 cells treated with cardiac glycosides, we found that it dropped substantially for all nine cardiac glycosides tested (Figure 3A). Similar results were obtained using both primary hepatocytes and iPSC-derived hepatocytes. These findings are not necessarily contradictory because if cardiac glycosides enhance the synthesis of cholesterol by hepatocytes, the degradation of apoB would prevent packaging into lipoprotein particles and the net effect would be a reduction in apoB secretion.

In heart failure and cardiac arrhythmia patients, glycosides act on cardiac myocytes by increasing the contractile force by inhibiting Na^+/K^+ -ATPase activity (Prassas and Diamandis, 2008). Inhibition of the Na^+/K^+ -ATPase disrupts the exchange of sodium and potassium ions across the plasma membrane, which indirectly increases intracellular calcium ions to promote contraction (Prassas and Diamandis, 2008). At this time, we do not know definitively whether cardiac glycosides also lower apoB production in hepatocytes by acting on the Na^+/K^+ -ATPase, but experiments are underway to address this hypothesis. We have shown that the downstream mechanism through which cardiac glycosides inhibit VLDL production is by promoting proteasome degradation of the apoB protein. However, the molecular relationship between the Na^+/K^+ -ATPase and intracellular apoB turnover remains speculative and could be multifactorial. The activity of the Na^+/K^+ -ATPase as an ion transporter is well established. However, more recent studies have shown that it also acts as a protein scaffold to support the assembly of a large signaling complex that includes SRC proto-oncogene, non-receptor tyrosine kinase (SRC) and the epidermal growth factor receptor (EGFR) (Prassas and Diamandis, 2008; Xie and Cai, 2003). Moreover, binding of cardiac glycosides to the Na^+/K^+ -ATPase can activate a number of cellular kinases, including mitogen-activated protein kinases (MAPK) and protein kinase C (PKC) (Xie and Cai, 2003). It is now, therefore, appreciated that cardiac glycosides can influence a broad repertoire of cell processes (Riganti et al., 2011; Newman et al., 2008; Prassas and Diamandis, 2008). Such processes include signal transduction, cell proliferation, glucose metabolism, Ca^{2+} flux, and steroid metabolism (Prassas and Diamandis, 2008). It would not be unreasonable to consider that some of these processes could intersect with lipoprotein processing.

Although cardiac glycosides have been used to treat heart failure for over 200 years, some clinicians have concerns over the narrow therapeutic window of the effective dosage and the fact that at high doses these drugs can cause severe arrhythmias and cardiac toxicity. However, the inhibition of Na^+/K^+ -ATPase activity in cardiac myocytes by cardiac glycosides most commonly requires micromolar concentrations (Werdan et al., 1984). In contrast, our results demonstrate that apoB production by hepatocytes is inhibited at nanomolar concentrations of glycosides. These results imply that the therapeutic dose needed to treat hypercholesterolemia by targeting the liver could

be lower than that needed to treat heart failure, thereby increasing efficacy and minimizing risk. Optimization of dosage could be determined by using humanized mice and by a controlled trial in patients. Efforts to address this are currently underway. Moreover, researchers have recently generated avatar mice using primary hepatocytes from an LDLR-deficient patient (Bissig-Choisat et al., 2015). Such mice could potentially be used to study the efficacy of cardiac glycosides in treating hoFH livers. Although further experiments are required to determine whether low doses of cardiac glycosides are efficacious, in the event that the optimum therapeutic dose used to lower LDL-C is similar to that used to treat cardiac dysfunction, cardiac toxicity could potentially be avoided by targeting the cardiac glycosides specifically to hepatocytes using small molecule drug conjugates (Wang et al., 2016).

In summary, we believe that our study adds to the potential therapeutic applications of the cardiac glycosides. Specifically, we propose that cardiac glycosides could be used to reduce LDL-C in individuals that are resistant or cannot tolerate statin treatment, which would include hoFH patients. Future study of the mechanisms through which the cardiac glycosides promote apoB turnover may also identify new pathways for the rational design of novel pharmaceuticals. More broadly, the approach that we have described highlights the feasibility of using iPSC-derived hepatocytes to identify treatments for inborn errors of hepatic metabolism in an academic setting. Coupled with the extensive availability of iPSCs from patients generated by the Next Generation Genetic Association Studies consortium, we believe that the relative cost-effectiveness and efficiency of this platform will facilitate an expansion in the discovery of small molecules and biologicals that can be used to treat rare diseases of the liver and cardiovascular system.

STAR METHODS

Detailed methods are provided in the online version of this paper and include the following:

- KEY RESOURCES TABLE
- CONTACT FOR REAGENT AND RESOURCE SHARING
- EXPERIMENTAL MODEL AND SUBJECT DETAILS
 - Pluripotent Stem Cells
 - Humanized FRGN Mice
 - Analysis of Human Patient Medical Records
- METHOD DETAILS
 - iPS Cell Differentiation
 - Drug Screen
 - Enzyme Linked Immunosorbent Assays (ELISA)
 - Lipoprotein characterization
 - Metabolic labeling, immunoprecipitation and western blot analyses
 - Quantitative Real-Time PCR analysis
- QUANTIFICATION AND STATISTICAL ANALYSIS

SUPPLEMENTAL INFORMATION

Supplemental Information includes three figures and one table and can be found with this article online at <http://dx.doi.org/10.1016/j.stem.2017.01.011>.

AUTHOR CONTRIBUTIONS

M.A.C. performed drug screens, cardiac glycoside characterizations, and data analyses; contributed to experimental design; and was responsible for the analysis of medical records. S.K.M. and F.K.N. contributed to the generation of humanized FRGN avatars and apoB analyses. F.D.F., R.J., A.U., and L.B.T. conducted studies on mechanisms of glycoside action, and M.D.G., M.C., and P.T. designed and performed protein synthesis studies. M.B. gave technical assistance with high-throughput screening. M.G. provided FRGN mice and advice on the production of avatars and experimental design. E.E.P. and D.J.R. designed and performed triglyceride labeling studies and contributed to data analyses, interpretation, and manuscript editing. W.Y. and E.E.M. contributed to the generation of iPSCs. S.A.D. contributed to data analyses, experimental design, and writing of the manuscript.

ACKNOWLEDGMENTS

This work was supported by the NIH grants DK55743, DK087377, DK102716 (S.A.D.), HG006398 (to S.A.D. and D.J.R.), and F30 DK091994 (to M.A.C.). Additional support was received from the Keck Foundation, the Phoebe R. and John D. Lewis Foundation, the Marcus Family, and the Sophia Wolf Quadracci Memorial Fund. Glenn Bushee provided valuable advice for the analyses of electronic medical records that was supported by the Medical College of Wisconsin CTSA grant 8UL1TR000055 and the Advancing a Healthier Wisconsin endowment at the Medical College of Wisconsin. Human hepatocytes were provided as a generous gift from Thermo Fisher Scientific, Life Technologies. Lisa Wilson and John Bial from the Yecuris Corporation provided expert advice and guidance in repopulation of FRGN mice with human hepatocytes. OHSU and Dr. Grompe have a significant financial interest in Yecuris, Inc., a company that may have a commercial interest in the results of this research and technology. This potential conflict of interest has been reviewed and managed by OHSU.

Received: November 7, 2016

Revised: December 22, 2016

Accepted: January 27, 2017

Published: April 6, 2017

REFERENCES

- Alphonse, P.A., and Jones, P.J. (2016). Revisiting human cholesterol synthesis and absorption: The reciprocity paradigm and its key regulators. *Lipids* 51, 519–536.
- Ambrosy, A.P., Butler, J., Ahmed, A., Vaduganathan, M., van Veldhuisen, D.J., Colucci, W.S., and Gheorghiade, M. (2014). The use of digoxin in patients with worsening chronic heart failure: reconsidering an old drug to reduce hospital admissions. *J. Am. Coll. Cardiol.* 63, 1823–1832.
- Asgari, S., Moslem, M., Bagheri-Lankarani, K., Pournasr, B., Miryounesi, M., and Baharvand, H. (2011). Differentiation and transplantation of human induced pluripotent stem cell-derived hepatocyte-like cells. *Stem Cell Rev.* 9, 493–504.
- Aslan, I., Kucuksayan, E., and Aslan, M. (2013). Effect of insulin analog initiation therapy on LDL/HDL subtraction profile and HDL associated enzymes in type 2 diabetic patients. *Lipids Health Dis.* 12, 54.
- Azuma, H., Pault, N., Ranade, A., Dorrell, C., Al-Dhalimy, M., Ellis, E., Strom, S., Kay, M.A., Finegold, M., and Grompe, M. (2007). Robust expansion of human hepatocytes in *Fah*^{-/-}/*Rag2*^{-/-}/*Il2rg*^{-/-} mice. *Nat. Biotechnol.* 25, 903–910.
- Basma, H., Soto-Gutiérrez, A., Yannam, G.R., Liu, L., Ito, R., Yamamoto, T., Ellis, E., Carson, S.D., Sato, S., Chen, Y., et al. (2009). Differentiation and transplantation of human embryonic stem cell-derived hepatocytes. *Gastroenterology* 136, 990–999.
- Berger, D.R., Ware, B.R., Davidson, M.D., Allsup, S.R., and Khetani, S.R. (2015). Enhancing the functional maturity of induced pluripotent stem cell-derived human hepatocytes by controlled presentation of cell-cell interactions *in vitro*. *Hepatology* 61, 1370–1381.

- Binda, D., Lasserre-Bigot, D., Bonet, A., Thomassin, M., Come, M.P., Guinchard, C., Bars, R., Jacqueson, A., and Richert, L. (2003). Time course of cytochromes P450 decline during rat hepatocyte isolation and culture: effect of L-NAME. *Toxicol. In Vitro* 17, 59–67.
- Bissig, K.D., Wieland, S.F., Tran, P., Isogawa, M., Le, T.T., Chisari, F.V., and Verma, I.M. (2010). Human liver chimeric mice provide a model for hepatitis B and C virus infection and treatment. *J. Clin. Invest.* 120, 924–930.
- Bissig-Choisat, B., Wang, L., Legras, X., Saha, P.K., Chen, L., Bell, P., Pankowicz, F.P., Hill, M.C., Barzi, M., Kettun Leyton, C., et al. (2015). Development and rescue of human familial hypercholesterolemia in a xenograft mouse model. *Nat. Commun.* 6, 7339.
- Cai, J., Zhao, Y., Liu, Y., Ye, F., Song, Z., Qin, H., Meng, S., Chen, Y., Zhou, R., Song, X., et al. (2007). Directed differentiation of human embryonic stem cells into functional hepatic cells. *Hepatology* 45, 1229–1239.
- Cameron, K., Tan, R., Schmidt-Heck, W., Campos, G., Lyall, M.J., Wang, Y., Lucendo-Villarin, B., Szkolnicka, D., Bates, N., Kimber, S.J., et al. (2015). Recombinant laminins drive the differentiation and self-organization of hESC-derived hepatocytes. *Stem Cell Reports* 5, 1250–1262.
- Campia, I., Gazzano, E., Pescarmona, G., Ghigo, D., Bosia, A., and Riganti, C. (2009). Digoxin and ouabain increase the synthesis of cholesterol in human liver cells. *Cell. Mol. Life Sci.* 66, 1580–1594.
- Cayo, M.A., Cai, J., DeLaForest, A., Noto, F.K., Nagaoka, M., Clark, B.S., Collery, R.F., Si-Tayeb, K., and Duncan, S.A. (2012). JD induced pluripotent stem cell-derived hepatocytes faithfully recapitulate the pathophysiology of familial hypercholesterolemia. *Hepatology* 56, 2163–2171.
- Choi, S.M., Kim, Y., Shim, J.S., Park, J.T., Wang, R.H., Leach, S.D., Liu, J.O., Deng, C., Ye, Z., and Jang, Y.Y. (2013). Efficient drug screening and gene correction for treating liver disease using patient-specific stem cells. *Hepatology* 57, 2458–2468.
- Cuchel, M., Bruckert, E., Ginsberg, H.N., Raal, F.J., Santos, R.D., Hegele, R.A., Kuivenhoven, J.A., Nordestgaard, B.G., Descamps, O.S., Steinhagen-Thiessen, E., et al.; European Atherosclerosis Society Consensus Panel on Familial Hypercholesterolemia (2014). Homozygous familial hypercholesterolemia: new insights and guidance for clinicians to improve detection and clinical management. A position paper from the Consensus Panel on Familial Hypercholesterolemia of the European Atherosclerosis Society. *Eur. Heart J.* 35, 2146–2157.
- Davidson, M.H. (2009). Novel nonstatin strategies to lower low-density lipoprotein cholesterol. *Curr. Atheroscler. Rep.* 11, 67–70.
- Davidson, M.D., Ware, B.R., and Khetani, S.R. (2015). Stem cell-derived liver cells for drug testing and disease modeling. *Discov. Med.* 19, 349–358.
- Davis, C.G., Lehrman, M.A., Russell, D.W., Anderson, R.G., Brown, M.S., and Goldstein, J.L. (1986). The J.D. mutation in familial hypercholesterolemia: amino acid substitution in cytoplasmic domain impedes internalization of LDL receptors. *Cell* 45, 15–24.
- Derwall, M., Malhotra, R., Lai, C.S., Beppu, Y., Aikawa, E., Seehra, J.S., Zapol, W.M., Bloch, K.D., and Yu, P.B. (2012). Inhibition of bone morphogenetic protein signaling reduces vascular calcification and atherosclerosis. *Arterioscler. Thromb. Vasc. Biol.* 32, 613–622.
- Ding, Q., Regan, S.N., Xia, Y., Oostrom, L.A., Cowan, C.A., and Musunuru, K. (2013). Enhanced efficiency of human pluripotent stem cell genome editing through replacing TALENs with CRISPRs. *Cell Stem Cell* 12, 393–394.
- Ebert, A.D., Yu, J., Rose, F.F.J., Jr., Mattis, V.B., Lorson, C.L., Thomson, J.A., and Svendsen, C.N. (2009). Induced pluripotent stem cells from a spinal muscular atrophy patient. *Nature* 457, 277–280.
- Ellis, E.C., Naugler, W.E., Parini, P., Mörk, L.M., Jorns, C., Zemack, H., Sandblom, A.L., Björkhem, I., Ericzon, B.G., Wilson, E.M., et al. (2013). Mice with chimeric livers are an improved model for human lipoprotein metabolism. *PLoS ONE* 8, e78550.
- Fagan, R.L., Wu, M., Chédin, F., and Brenner, C. (2013). An ultrasensitive high throughput screen for DNA methyltransferase 1-targeted molecular probes. *PLoS ONE* 8, e78752.
- Fisher, E.A., and Ginsberg, H.N. (2002). Complexity in the secretory pathway: the assembly and secretion of apolipoprotein B-containing lipoproteins. *J. Biol. Chem.* 277, 17377–17380.
- Gayathri, V., Ananthi, S., Chandronitha, C., Sangeetha, M.K., and Vasanthi, H.R. (2011). Hypolipidemic potential of flowers of *Nerium oleander* in high fat diet-fed Sprague Dawley rats. *Nat. Prod. Res.* 25, 1110–1114.
- Ginsberg, H.N., and Fisher, E.A. (2009). The ever-expanding role of degradation in the regulation of apolipoprotein B metabolism. *J. Lipid Res.* 50 (Suppl.), S162–S166.
- Hay, D.C., Zhao, D., Fletcher, J., Hewitt, Z.A., McLean, D., Urruticoechea-Uriguen, A., Black, J.R., Elcombe, C., Ross, J.A., Wolf, R., and Cui, W. (2008). Efficient differentiation of hepatocytes from human embryonic stem cells exhibiting markers recapitulating liver development in vivo. *Stem Cells* 26, 894–902.
- Horvath, P., Aulner, N., Bickle, M., Davies, A.M., Nery, E.D., Ebner, D., Montoya, M.C., Östling, P., Pietiäinen, V., Price, L.S., et al. (2016). Screening out irrelevant cell-based models of disease. *Nat. Rev. Drug Discov.* 15, 751–769.
- Hothi, S.S., Chinnappa, S., and Tan, L.B. (2013). 200+ years of a misunderstood drug for treating chronic heart failure: digoxin, why and how should we continue using it? *Int. J. Cardiol.* 168, 645–647.
- Jonker, J.T., Wang, Y., de Haan, W., Diamant, M., Rijzewijk, L.J., van der Meer, R.W., Lamb, H.J., Tamsma, J.T., de Roos, A., Romijn, J.A., et al. (2010). Pioglitazone decreases plasma cholestryl ester transfer protein mass, associated with a decrease in hepatic triglyceride content, in patients with type 2 diabetes. *Diabetes Care* 33, 1625–1628.
- Kimbrel, E.A., and Lanza, R. (2015). Current status of pluripotent stem cells: moving the first therapies to the clinic. *Nat. Rev. Drug Discov.* 14, 681–692.
- Kocisko, D.A., Baron, G.S., Rubenstein, R., Chen, J., Kuizon, S., and Caughey, B. (2003). New inhibitors of scrapie-associated prion protein formation in a library of 2000 drugs and natural products. *J. Virol.* 77, 10288–10294.
- Kolkhof, P., Geerts, A., Schäfer, S., and Torzewski, J. (2010). Cardiac glycosides potently inhibit C-reactive protein synthesis in human hepatocytes. *Biochem. Biophys. Res. Commun.* 394, 233–239.
- Lang, J., Vera, D., Cheng, Y., and Tang, H. (2016). Modeling dengue virus-hepatocyte interactions using human pluripotent stem cell-derived hepatocyte-like cells. *Stem Cell Reports* 7, 341–354.
- Lee, G., Papapetrou, E.P., Kim, H., Chambers, S.M., Tomishima, M.J., Fasano, C.A., Ganat, Y.M., Menon, J., Shimizu, F., Viale, A., et al. (2009). Modelling pathogenesis and treatment of familial dysautonomia using patient-specific iPSCs. *Nature* 461, 402–406.
- Leung, A., Nah, S.K., Reid, W., Ebata, A., Koch, C.M., Monti, S., Genereux, J.C., Wiseman, R.L., Wolozin, B., Connors, L.H., et al. (2013). Induced pluripotent stem cell modeling of multisystemic, hereditary transthyretin amyloidosis. *Stem Cell Reports* 1, 451–463.
- Li, S., Guo, J., Ying, Z., Chen, S., Yang, L., Chen, K., Long, Q., Qin, D., Pei, D., and Liu, X. (2015). Valproic acid-induced hepatotoxicity in Alpers syndrome is associated with mitochondrial permeability transition pore opening-dependent apoptotic sensitivity in an induced pluripotent stem cell model. *Hepatology* 61, 1730–1739.
- Liang, J., Wu, X., Jiang, H., Zhou, M., Yang, H., Angkeow, P., Huang, L.S., Sturley, S.L., and Ginsberg, H. (1998). Translocation efficiency, susceptibility to proteasomal degradation, and lipid responsiveness of apolipoprotein B are determined by the presence of beta sheet domains. *J. Biol. Chem.* 273, 35216–35221.
- Ludwig, T.E., Bergendahl, V., Levenstein, M.E., Yu, J., Probasco, M.D., and Thomson, J.A. (2006). Feeder-independent culture of human embryonic stem cells. *Nat. Methods* 3, 637–646.
- Maetzel, D., Sarkar, S., Wang, H., Abi-Mosleh, L., Xu, P., Cheng, A.W., Gao, Q., Mitalipova, M., and Jaenisch, R. (2014). Genetic and chemical correction of cholesterol accumulation and impaired autophagy in hepatic and neural cells derived from Niemann-Pick Type C patient-specific iPS cells. *Stem Cell Reports* 2, 866–880.

- Mallanna, S.K., and Duncan, S.A. (2013). Differentiation of hepatocytes from pluripotent stem cells. *Curr. Protoc. Stem Cell Biol.* 26, 1G.4.1–1G.4.13.
- Mallanna, S.K., Cayo, M.A., Twaroski, K., Gundry, R.L., and Duncan, S.A. (2016). Mapping the cell-surface N-glycoproteome of human hepatocytes reveals markers for selecting a homogeneous population of iPSC-derived hepatocytes. *Stem Cell Reports* 7, 543–556.
- Matsa, E., Burridge, P.W., and Wu, J.C. (2014). Human stem cells for modeling heart disease and for drug discovery. *Sci. Transl. Med.* 6, 239ps6.
- Nagiec, M.M., Skepner, A.P., Negri, J., Eichhorn, M., Kuperwasser, N., Comer, E., Muncipinto, G., Subramanian, A., Clish, C., Musunuru, K., et al. (2015). Modulators of hepatic lipoprotein metabolism identified in a search for small-molecule inducers of tribbles pseudokinase 1 expression. *PLoS ONE* 10, e0120295.
- Newman, R.A., Yang, P., Pawlus, A.D., and Block, K.I. (2008). Cardiac glycosides as novel cancer therapeutic agents. *Mol. Interv.* 8, 36–49.
- Nissen, S.E., Dent-Acosta, R.E., Rosenson, R.S., Stroes, E., Sattar, N., Preiss, D., Mancini, G.B., Ballantyne, C.M., Catapano, A., Gouni-Berthold, I., et al.; GAUSS-3 Investigators (2016). Comparison of PCSK9 inhibitor evolocumab vs ezetimibe in statin-intolerant patients: Design of the goal achievement after utilizing an anti-PCSK9 antibody in statin-intolerant subjects 3 (GAUSS-3) trial. *Clin. Cardiol.* 39, 137–144.
- Prassas, I., and Diamandis, E.P. (2008). Novel therapeutic applications of cardiac glycosides. *Nat. Rev. Drug Discov.* 7, 926–935.
- Rader, D.J., and Kastelein, J.J. (2014). Lomitapide and mipomersen: two first-in-class drugs for reducing low-density lipoprotein cholesterol in patients with homozygous familial hypercholesterolemia. *Circulation* 129, 1022–1032.
- Rader, D.J., Cohen, J., and Hobbs, H.H. (2003). Monogenic hypercholesterolemia: new insights in pathogenesis and treatment. *J. Clin. Invest.* 111, 1795–1803.
- Rashid, S.T., Corbineau, S., Hannan, N., Marciniak, S.J., Miranda, E., Alexander, G., Huang-Doran, I., Griffin, J., Ahrlund-Richter, L., Skepper, J., et al. (2010). Modeling inherited metabolic disorders of the liver using human induced pluripotent stem cells. *J. Clin. Invest.* 120, 3127–3136.
- Riganti, C., Campia, I., Kopecka, J., Gazzano, E., Doublier, S., Aldieri, E., Bosia, A., and Ghigo, D. (2011). Pleiotropic effects of cardioactive glycosides. *Curr. Med. Chem.* 18, 872–885.
- Robinton, D.A., and Daley, G.Q. (2012). The promise of induced pluripotent stem cells in research and therapy. *Nature* 481, 295–305.
- Schwartz, R.E., Trehan, K., Andrus, L., Sheahan, T.P., Ploss, A., Duncan, S.A., Rice, C.M., and Bhatia, S.N. (2012). Modeling hepatitis C virus infection using human induced pluripotent stem cells. *Proc. Natl. Acad. Sci. USA* 109, 2544–2548.
- Si-Tayeb, K., Noto, F.K., Nagaoka, M., Li, J., Battle, M.A., Duris, C., North, P.E., Dalton, S., and Duncan, S.A. (2010a). Highly efficient generation of human hepatocyte-like cells from induced pluripotent stem cells. *Hepatology* 51, 297–305.
- Si-Tayeb, K., Noto, F.K., Sepac, A., Sedlic, F., Bosnjak, Z.J., Lough, J.W., and Duncan, S.A. (2010b). Generation of human induced pluripotent stem cells by simple transient transfection of plasmid DNA encoding reprogramming factors. *BMC Dev. Biol.* 10, 81.
- Song, Z., Cai, J., Liu, Y., Zhao, D., Yong, J., Duo, S., Song, X., Guo, Y., Zhao, Y., Qin, H., et al. (2009). Efficient generation of hepatocyte-like cells from human induced pluripotent stem cells. *Cell Res.* 19, 1233–1242.
- Strittmatter, S.M. (2014). Overcoming drug development bottlenecks with repurposing: Old drugs learn new tricks. *Nat. Med.* 20, 590–591.
- Sullivan, G.J., Hay, D.C., Park, I.H., Fletcher, J., Hannoun, Z., Payne, C.M., Dalgetty, D., Black, J.R., Ross, J.A., Samuel, K., et al. (2010). Generation of functional human hepatic endoderm from human induced pluripotent stem cells. *Hepatology* 51, 329–335.
- Sundaram, M., and Yao, Z. (2010). Recent progress in understanding protein and lipid factors affecting hepatic VLDL assembly and secretion. *Nutr. Metab. (Lond.)* 7, 35.
- Szkołnicka, D., Lucendo-Villarin, B., Moore, J.K., Simpson, K.J., Forbes, S.J., and Hay, D.C. (2016). Reducing hepatocyte injury and necrosis in response to paracetamol using noncoding RNAs. *Stem Cells Transl. Med.* 5, 764–772.
- Tafaleng, E.N., Chakraborty, S., Han, B., Hale, P., Wu, W., Soto-Gutierrez, A., Feghali-Bostwick, C.A., Wilson, A.A., Kotton, D.N., Nagaya, M., et al. (2015). Induced pluripotent stem cells model personalized variations in liver disease resulting from α 1-antitrypsin deficiency. *Hepatology* 62, 147–157.
- Takahashi, K., Tanabe, K., Ohnuki, M., Narita, M., Ichisaka, T., Tomoda, K., and Yamanaka, S. (2007). Induction of pluripotent stem cells from adult human fibroblasts by defined factors. *Cell* 131, 861–872.
- Thompson, P.D., Clarkson, P., and Karas, R.H. (2003). Statin-associated myopathy. *JAMA* 289, 1681–1690.
- Touboul, T., Hannan, N.R., Corbineau, S., Martinez, A., Martinet, C., Branchereau, S., Mainot, S., Strick-Marchand, H., Pedersen, R., Di Santo, J., et al. (2010). Generation of functional hepatocytes from human embryonic stem cells under chemically defined conditions that recapitulate liver development. *Hepatology* 51, 1754–1765.
- Wang, C., Tao, W., Wang, Y., Bikow, J., Lu, B., Keating, A., Verma, S., Parker, T.G., Han, R., and Wen, X.Y. (2010). Rosuvastatin, identified from a zebrafish chemical genetic screen for antiangiogenic compounds, suppresses the growth of prostate cancer. *Eur. Urol.* 58, 418–426.
- Wang, Y., Cheetham, A.G., Angacian, G., Su, H., Xie, L., and Cui, H. (2016). Peptide-drug conjugates as effective prodrug strategies for targeted delivery. *Adv. Drug Deliv. Rev.*, S0169–409X(16)30208-3.
- Weisman, J.L., Liou, A.P., Shelat, A.A., Cohen, F.E., Guy, R.K., and DeRisi, J.L. (2006). Searching for new antimalarial therapeutics amongst known drugs. *Chem. Biol. Drug Des.* 67, 409–416.
- Werdan, K., Wagenknecht, B., Zwissler, B., Brown, L., Krawietz, W., and Erdmann, E. (1984). Cardiac glycoside receptors in cultured heart cells—I. Characterization of one single class of high affinity receptors in heart muscle cells from chick embryos. *Biochem. Pharmacol.* 33, 55–70.
- Wilson, E.M., Bial, J., Tarlow, B., Bial, G., Jensen, B., Greiner, D.L., Brehm, M.A., and Grompe, M. (2014). Extensive double humanization of both liver and hematopoiesis in FRGN mice. *Stem Cell Res. (Amst.)* 13 (3 Pt A), 404–412.
- Xie, Z., and Cai, T. (2003). Na⁺-K⁺-ATPase-mediated signal transduction: from protein interaction to cellular function. *Mol. Interv.* 3, 157–168.
- Yang, W., Liu, Y., Slovik, K.J., Wu, J.C., Duncan, S.A., Rader, D.J., and Morrisey, E.E. (2015). Generation of iPSCs as a pooled culture using magnetic activated cell sorting of newly reprogrammed cells. *PLoS One* 10, e0134995.
- Yi, F., Qu, J., Li, M., Suzuki, K., Kim, N.Y., Liu, G.H., and Belmonte, J.C. (2012). Establishment of hepatic and neural differentiation platforms of Wilson's disease specific induced pluripotent stem cells. *Protein Cell* 3, 855–863.
- Yu, J., Vodyanik, M.A., Smuga-Otto, K., Antosiewicz-Bourget, J., Frane, J.L., Tian, S., Nie, J., Jonsdottir, G.A., Ruotti, V., Stewart, R., et al. (2007). Induced pluripotent stem cell lines derived from human somatic cells. *Science* 318, 1917–1920.
- Zhang, X.D. (2011). Illustration of SSMD, z score, SSMD*, z* score, and t statistic for hit selection in RNAi high-throughput screens. *J. Biomol. Screen.* 16, 775–785.
- Zhang, S., Chen, S., Li, W., Guo, X., Zhao, P., Xu, J., Chen, Y., Pan, Q., Liu, X., Zychlinski, D., et al. (2011). Rescue of ATP7B function in hepatocyte-like cells from Wilson's disease induced pluripotent stem cells using gene therapy or the chaperone drug curcumin. *Hum. Mol. Genet.* 20, 3176–3187.

STAR★METHODS

KEY RESOURCES TABLE

REAGENT or RESOURCE	SOURCE	IDENTIFIER
Antibodies		
anti-FLAG M2	Sigma-Aldrich	F3165; RRID: AB_259529
human albumin	Bethyl Laboratories	A80-129A
HRP conjugated human albumin	Bethyl Laboratories	A80-129P
3,3',5,5'-tetramethylbenzidine (TMB)	Bethyl Laboratories	RS10-110
human apoB	MabTech, Inc.	3715-1H-6
anti-human apoB mAbs LDL 17/20	MabTech, Inc.	3715-3-250; RRID: AB_907207
HSP90 β	Abcam	ab32568; RRID: AB_733044
Goat anti-Mouse IgG	Thermo Fisher Scientific	31430; RRID: AB_228307
Goat Anti-Rabbit IgG	Thermo Fisher Scientific	656120; RRID: AB_2533967
Biological Samples		
pzbFGF BL21 Star <i>E. coli</i>	Teneille Ludwig	Ludwig et al., 2006
Chemicals, Peptides, and Recombinant Proteins		
B-27 Supplement (50X), serum free	Thermo Fisher Scientific	17504044
B-27 Supplement, minus insulin	Thermo Fisher Scientific	A1895601
Activin A Recombinant Human Protein	Thermo Fisher Scientific	PHC9563
FGF-Basic (AA 10-155) Recombinant Human Protein	Thermo Fisher Scientific	PHG0023
Purified recombinant zebrafish FGF-Basic	Duncan Lab	Ludwig et al., 2006
BMP4 Recombinant Human Protein	Thermo Fisher Scientific	PHC9533
HGF Recombinant Human Protein	Thermo Fisher Scientific	PHG0321
Oncostatin M Recombinant Human Protein	Thermo Fisher Scientific	PHC5015
Gitoxin	MicroSource Discovery Systems, Inc.	Spectrum Collection; CAS 4562-36-1
Peruvoside	MicroSource Discovery Systems, Inc.	01501113; CAS 1182-67-2
Strophanthidin	MicroSource Discovery Systems, Inc.	00100291; CAS 66-28-4
Lanatoside C	MicroSource Discovery Systems, Inc.	01501205; CAS 7575-22-3
Convallatoxin	MicroSource Discovery Systems, Inc.	01503994; CAS 508-75-8
Selamectin	MicroSource Discovery Systems, Inc.	Spectrum Collection; CAS 165108-07-6
Hycanthone	MicroSource Discovery Systems, Inc.	Spectrum Collection; 3105-97-3
Donepezil Hydrochloride	MicroSource Discovery Systems, Inc.	Spectrum Collection; 142057-77-0
Digitoxin	MicroSource Discovery Systems, Inc.	01500246; CAS 71-63-6
Proscillarin	Santa Cruz Biotechnology	sc-500903; CAS 466-06-8
Digoxin	MicroSource Discovery Systems, Inc.	Spectrum Collection; 20830-75-5
Sulfachloropyridazine	MicroSource Discovery Systems, Inc.	Spectrum Collection; 80-32-0
Tetroquinone	MicroSource Discovery Systems, Inc.	Spectrum Collection; CAS 319-89-1
Phenylmercuric acetate	MicroSource Discovery Systems, Inc.	Spectrum Collection; CAS 62-38-4
Methscopolamine bromide	MicroSource Discovery Systems, Inc.	Spectrum Collection; CAS 155-41-9
Famciclovir	MicroSource Discovery Systems, Inc.	Spectrum Collection; CAS 104227-87-4
Ouabain Octahydrate	MicroSource Discovery Systems, Inc.	01500676; CAS 11018-89-6, 630-60-4
Cycloheximide	Sigma-Aldrich	C1988; CAS 66-81-9
MG132	Selleck Chemicals	S2619; CAS 133407-82-6
Dimethyl sulfoxide	Sigma-Aldrich	D8418; CAS 67-68-5
CuRx Nitisinone	Yecuris Corporation	20-0027; CAS 104206-65-7
Critical Commercial Assays		
RNeasy mini Kit	QIAGEN	74106
TURBO DNA-free Kit	Thermo Fisher/Ambion	AM1907

(Continued on next page)

Continued

REAGENT or RESOURCE	SOURCE	IDENTIFIER
M-MLV Reverse Transcriptase	Thermo Fisher/Invitrogen	28025-013
TaqMan Gene Expression	Thermo Fisher/Applied Biosystems	4369016
Power SYBR Green	Thermo Fisher/Applied Biosystems	4367659
Human apoB ELISA development kit (HRP)	MabTech, Inc.	3715-1H-20
Experimental Models: Cell Lines		
HoFH iPSC-JD4	Stephen Duncan	Cayo et al., 2012
Wild type iPSC-K3	Stephen Duncan	Si-Tayeb et al., 2010b
Wild type iPSC-SV20	Wenli Yang	Yang et al., 2015
Female Primary Hepatocytes	Thermo Fisher/Life Technologies	#Hu1475
Male Primary Hepatocytes	Celsis In Vitro Technologies/ Bioreclamation, LLC	#M00995
HepG2 cells	ATCC	#HB-8065
Experimental Models: Organisms/Strains		
Mouse: <i>Frgn</i> ; <i>Fah</i> ^{-/-} / <i>Rag2</i> ^{-/-} / <i>Il2rg</i> ^{-/-} NOD	Markus Grompe	Wilson et al., 2014
Sequence-Based Reagents		
Primer Assay apoB	Integrated DNA Technologies	Hs.PT.47.18897448
56-FAM/CT GGA TAC C/Zen/G TGT ATG GAA ACT GCT CC/3IABkFQ/	Integrated DNA Technologies	Hs.PT.47.18897448
Primer 1-CAT TGC CCT TCC TCG TCT T	Integrated DNA Technologies	Hs.PT.47.18897448
Primer 2-CCA GAG ACA GAA GAA GCC AAG	Integrated DNA Technologies	Hs.PT.47.18897448
Primer Assay rpl13	Integrated DNA Technologies	Hs.PT.58.1788586
56-FAM/AGCAGTACC/ZEN/TGTTTAGGCCACGATGG/ 3IABkFQ	Integrated DNA Technologies	Hs.PT.58.1788586
Primer 1-GCCTTCACAGCGTACGA	Integrated DNA Technologies	Hs.PT.58.1788586
Primer 2-CGAAGATGGCGGAGGTG	Integrated DNA Technologies	Hs.PT.58.1788586
Software and Algorithms		
Microsoft Excel for Mac v15.29	Microsoft	
Adobe Illustrator CS6	Adobe Systems Inc.	
Adobe Photoshop CS6	Adobe Systems Inc.	
Image Lab software	Bio-Rad	1709691
Graphpad Prism v6	Graphpad Software, Inc.	
Other		
Spectrum Collection	Microsource Discovery Systems Inc.	http://www.msdiscovery.com/spectrum.html
Hepatocyte Thaw Medium	Thermo Fisher Scientific	CM7500
Williams' Medium E	Sigma-Aldrich	W4128
HCM BulletKit (CC-3199 & CC-4182)	Lonza	CC-3198

CONTACT FOR REAGENT AND RESOURCE SHARING

Further information and requests for reagents may be directed to, and will be fulfilled by, the Lead Contact, Dr. Stephen A. Duncan (duncanst@musc.edu).

EXPERIMENTAL MODEL AND SUBJECT DETAILS**Pluripotent Stem Cells**

The MCW SCRO committee approved all human iPSC work (hSCRO approval #09-005). All iPSCs were produced by us and their characterization has been described elsewhere (Si-Tayeb et al., 2010b; Cayo et al., 2012). JD4 iPSCs were generated from primary dermal fibroblasts (GM02408) from a compound heterozygote familial hypercholesterolemia patient that were provided by the Coriell Institute for Medical Research (Coriell Cell Repositories, Camden, NJ) (Cayo et al., 2012). Control K3 iPSCs were produced from foreskin fibroblasts (CRL2097) obtained from ATCC (Si-Tayeb et al., 2010b).

Humanized FRGN Mice

The MCW IACUC approved all animal experiments. *Fah^{-/-} Rag2^{-/-} IL2gr^{-/-}* NOD (FRGN) mice were generated by Dr. Markus Grompe (Azuma et al., 2007; Wilson et al., 2014). Breeding colonies of FRGN mice were maintained on water supplemented with 8 mg/L NTBC. To generate avatars, 1×10^6 human primary hepatocytes were introduced into 6-8 week-old male FRGN mice by splenic injection. NTBC was withdrawn from the drinking water and mice were left for 7 days. Mice were then transferred to 8 mg/L NTBC for 3 days. The mice were cycled 7 days off drug followed by 3 days on drug for 2 months. After 2 months of cycling mice were kept without NTBC for around 15 days or until they had lost 15% of body weight at which point they were returned to NTBC for 4 days. This cycle was maintained for the life of the animal. The extent of engraftment was measured by determining the human serum albumin by ELISA, as described (Azuma et al., 2007; Bissig et al., 2010; Ellis et al., 2013). We also confirmed that antibodies used to detect apoB specifically detected the human and not mouse forms of the protein (Figure S2A), levels of human apoB in the serum correlated with the level of human albumin (Figure S2B), and engraftment and expansion of human hepatocytes recapitulated published results (Azuma et al., 2007; Wilson et al., 2014) by immunostaining liver sections for human albumin, FAH, and human trans Golgi network protein 46 (TGN46) (Figure S2C). Human hepatocytes for transplantation were obtained either from Thermo Fisher/Life Technologies (donor A, Hu1475) or from Celsis In Vitro Technologies, INC (donor B). Donor A was a 53 year old, Caucasian female whose cause of death was unknown, occasionally used alcohol (wine, 2 glasses daily) and was an ex-smoker (1 ppd x 30 years, stopped in 2007). Donor B was a 17yr old Caucasian who died from head trauma due to a motor vehicle accident who occasionally used alcohol and dipping tobacco. For drug treatment studies, highly repopulated FRGN mice ($> 1\text{mg/ml}$ serum human albumin) were maintained using 0.15mg/L NTBC drinking water prior to and during 48 hr drug treatment experiments. Blood samples were collected using 4mm Goldenrod animal lancets (Medipoint, Inc.) and BD Microtainer EDTA-coated plasma collection tubes (Becton Dickinson Vacutainer Systems). Serum samples were collected at times 0, 24, and 48 hr. Mice were weighed daily, and treated with either 0.5 mg/kg digoxin, 0.6 mg/kg proscillarin or vehicle control (5% DMSO in sterile saline) by i.p. injection at time points 0, 16, and 40 hr. Serum concentrations of human albumin and human apoB were determined using ELISA.

Analysis of Human Patient Medical Records

All medical records were de-identified and considered exempt non-human subjects research. Access to de-identified medical records was approved through an MCW Clinical & Translational Research Data Use Agreement and records were obtained through an honest broker. The Froedtert/MCW Hospital and Clinics Epic Systems electronic medical record was queried using the MCW i2b2 Clinical & Translational Research Informatics Data Warehouse (CTRI-CRDW), and Cohort Discovery Tool. A cohort of patients was identified whose charts included at least one medication order for a cardiac glycoside (n = 5,493). From this cohort of patients, we extracted de-identified medical records data pertinent to our research hypotheses, specifically, serum LDL-C (direct) and serum albumin concentration clinical laboratory results, and medication (cardiac glycosides, statin, and ACE-inhibitor) orders (start/end dates). Laboratory test results (LDL-C, albumin) were flagged as 'on-drug' or 'off-drug' (cardiac glycoside, statin, and ACE-inhibitor) using the medication orders data (start/end dates) for each individual patient. If a patient's records contained multiple laboratory result values within a single on-drug or off-drug window, the multiple values were combined into an average, such that each data point represents a patient's average laboratory value for the time window. Final cohorts used for analysis are as follows: Patients with LDL-C measurements treated with an ACE-inhibitor ('on' n = 180; 'off' n = 165), a statin ('on' n = 221; 'off' n = 204), or a cardiac glycoside ('on' n = 324; 'off' n = 205). Patients with albumin measurements treated with an ACE-inhibitor ('on' n = 1767; 'off' n = 763), a statin ('on' n = 1865; 'off' n = 906), or a cardiac glycoside ('on' n = 2116; 'off' n = 770). From within the larger cohorts, we identified a series of patients treated with a cardiac glycoside (n = 21) or a statin (n = 20) with matched LDL-C measurements 'on drug' and 'off drug' for direct comparison. An identical group was developed for statin (n = 715) or cardiac glycoside (n = 87) treated patients with matched albumin measurements.

Data inclusion/exclusion criteria: For direct LDL-C, any laboratory test results with values below 30 mg/dL were excluded (3 of 1,192 total), along with 4 results that were flagged as 'error' within the patients' charts. For albumin, any tests flagged with 'error' were also excluded, as were pathological results < 3 or > 5.4 g/dL (4,333 of total 59,532 lab results). Statistical significance of all results was determined using Student's t tests. Paired data for individual patients on-drug versus off-drug was analyzed using paired t tests.

METHOD DETAILS

iPS Cell Differentiation

A step-by-step protocol that we used to differentiate human iPSCs into hepatocyte-like cells has been published elsewhere (Mal-lanna and Duncan, 2013; Si-Tayeb et al., 2010a). Specifically, iPSCs were plated as monolayers in 96-well plates. The cells were induced to form endoderm by addition of 100 ng/ml Activin A for 5 days. Endoderm was then converted to hepatic progenitor cells by addition of Bone Morphogenetic Protein 4 (BMP4 20 ng/ml) and Fibroblast Growth Factor 2 (FGF2 10 ng/ml) for a further 5 days. Immature hepatocytes were generated by inclusion of Hepatocyte Growth Factor (HGF 20 ng/ml) and cells were induced to mature by addition of Oncostatin M (OSM 20 ng/ml) each for 5 days.

Drug Screen

HoFH iPSC-JD4 cells were differentiated to hepatocyte-like cells in 96-well plates. A 24 hr pre-drug treatment sample of medium was retained before the addition of drugs from the SPECTRUM collection drug library for 24 hr at 5 μ M. ApoB concentrations were determined for each compound in the small molecule library using a standard curve and four parameter logistic (4PL) regression model in both pre- and post-drug treated samples by ELISA. The pre-drug and post-drug apoB concentrations were combined and expressed as a delta-apoB ratio (post-drug [apoB]:pre-drug [apoB]), and a z-score was generated for each individual compound using the delta-apoB ratio with the standard deviation of the delta-apoB ratios from the parent drug plate (30 drug plates total). Primary hits were validated in secondary replicate experiments (biological replicates n = 3), and statistical significance was determined by a Student's t test. The SPECTRUM collection drug library was purchased from Microsource Discovery Systems INC. The library consists of 2320 small molecules (<http://www.msdiscovery.com/spectrum.html>) and has been previously used to identify drugs for repurposing (Weisman et al., 2006; Kocisko et al., 2003; Fagan et al., 2013; Wang et al., 2010).

Enzyme Linked Immunosorbent Assays (ELISA)

A sandwich ELISA to detect human albumin in tissue culture supernatants and mouse sera used a 1/100 dilution of a capture human albumin coating antibody (Bethyl laboratories, A80-129A) and a 1:85,000 dilution of a Horseradish Peroxidase (HRP) conjugated human albumin detection antibody (Bethyl laboratories, A80-129P). Bound antibody was detected using 3,3',5,5'-tetramethylbenzidine (TMB) and the concentration of albumin in each sample determined by comparing to a standard curve (Bethyl laboratories, RS10-110). Human apoB was detected using a commercial sandwich ELISA (product code: 3715-1H-6; MabTech, Inc) and detected using TMB. The concentration of apoB was determined by comparing to a standard curve using apoB supplied by the manufacturer. This assay has been used to quantify human apoB levels in serum and cell culture medium previously (Aslan et al., 2013; Derwall et al., 2012; Jonker et al., 2010).

Lipoprotein characterization

Primary human hepatocytes were plated on collagen coated dishes in Hepatocyte Thaw Medium (ThermoFisher) for 4-6 hr before medium was changed to William's E medium (ThermoFisher) with and without DMSO, digoxin (310 nM) or proscillaridin (310 nM). After an overnight incubation, triglycerides were labeled with [³H]-glycerol (10 μ Ci/ml) conjugated oleate in William's E medium supplemented with DMSO, digoxin (310 nM) or proscillaridin (310 nM) for 4 hr using standard procedures. The conditioned media was filtered through a 0.45 um filter to remove cell debris, concentrated on a centrifugal cellulose membrane (EMD Millipore), and fractionated by FPLC.

Metabolic labeling, immunoprecipitation and western blot analyses

iPSC-derived hepatocytes (day 20) and undifferentiated iPSCs were treated with DMSO or digoxin (310 nM) overnight. Cells were then incubated for 30 min with methionine free DMEM medium before labeling for 60 min with [³⁵S]-Met \pm digoxin (310 nm). Immunoprecipitation of cell lysates was performed using anti-ApoB (MabTech LDL 17/20) and anti-FLAG M2 antibody (SIGMA). After SDS-PAGE using a 4%-15% acrylamide gradient, gels were exposed to a phosphorimager screen and developed using a FLA 9000 Typhoon Storage Phosphorimager (GE Healthcare). For western blots iPSC-derived hepatocytes (day 20) were treated between 8 – 24 hr, depending on the experiment, with DMSO, cycloheximide (100 μ M), digoxin (310 nM), proscillaridin (310 nM), MG132 (10 μ M), or combinations of these drugs. Protein concentration was determined by BCA assay (Bio-Rad) and 30 μ g of protein separated by SDS-PAGE using Any kD™ Mini-protean TGX stain-free™ precast gels (BioRad, CA, #4568123), and transferred to PVDF membranes using the Trans-Blot Turbo™ Transfer System (BioRad, CA, #1704155). Membranes were probed with anti-ApoB (MabTech LDL 17/20) and detected using HRP-conjugated secondary antibodies. Protein levels were calculated using the stain-free Imaging System (Bio-Rad) and were normalized to total protein using Image Lab software (Bio-Rad).

Quantitative Real-Time PCR analysis

RNA was isolated from drug-treated and control iPSC-derived hepatocyte-like cells using the RNeasy mini Kit (QIAGEN, #74106). Genomic DNA was removed using the TURBO DNA-free™ Kit (ThermoFisher/Ambion, NY, #AM1907). First strand cDNA was synthesized using M-MLV Reverse Transcriptase (ThermoFisher/Invitrogen, NY, #28025-013). Quantitative real-time PCR was performed on a BioRad CFX384 real-time PCR machine.

QUANTIFICATION AND STATISTICAL ANALYSIS

Figure 1: Data points in panels A, B, D, and E represent independent wells (n = 1 well per point), from 96-well cell culture plates. For z' calculation in panel A, n = 107 wells for each of the 2 groups of measurements (iPSC-derived hepatocytes, iPSC-derived endoderm). For panel B, statistical significance was determined using a Student's t test. In panel D, each plate is represented by a boxplot and 80 data points representing the 80 drug compounds contained on that plate. Figures and statistics were generated using Microsoft Excel and R.

Figure 2: In panel A, each data point represents the mean and SD (error bars) of 3 independent wells (n = 3 wells per point) from 96-well cell culture plates. Statistical significance reported in panel C was determined using a Student's t test. Graphs and statistics were generated using GraphPad Prism and Microsoft Excel.

Figure 3: In panel A, each data point represents the mean \pm SEM (error bars) of 3 independent wells ($n = 3$ wells per point) from a 96-well cell culture plate. In panel B, each bar represents the mean \pm SEM (error bars) of 3 independent wells ($n = 3$ wells per bar) from a 96-well cell culture plate. Graphs were generated using Microsoft Excel.

Figure 4: In panel B, data points represent mean \pm SEM (error bars) of 2 independent wells ($n = 2$ wells per point) from a 12-well cell culture plate. Panel C data are from 4 independent wells collected from two independent differentiations and error bars represent SEM. Panel D shows results of metabolic labeling analyses of apoB that is representative of 3 independent differentiations. Panel E is a micrograph showing an immunoblot analysis that is representative of results obtained from 3 independent differentiations of iPSC3 cells. Similar results were obtained from iPSC SV20 cells when measured at 8 hr of treatment. Panel F contains data from three independent differentiations and error bars represent SEM. Panel G immunoblot is representative of 4 independent differentiations and panel H shows quantification of blots with error bars representing SEM. Where appropriate significance was calculated using Student's t test.

Figure 5: In panels A&B, each data point represents a single clinical laboratory result (or the mean result value for patients with multiple laboratory results), and horizontal lines represent the mean laboratory result value for the indicated group of data points. Panel A: ACE inhibitor ('on' $n = 180$, 'off' $n = 165$); statin ('on' $n = 221$, 'off' $n = 204$); cardiac glycoside ('on' $n = 324$, 'off' $n = 205$). Panel B: ACE inhibitor ('on' $n = 1767$, 'off' $n = 763$); statin ('on' $n = 1865$, 'off' $n = 906$); cardiac glycoside ('on' $n = 2116$, 'off' $n = 770$). Statistical significance was determined using unpaired Student's t tests. In panels C&D, data points represent a single clinical laboratory result (or the mean result value for patients with multiple laboratory results), and are paired such that each 'on-drug' data point has a single corresponding 'off-drug' point. Horizontal lines represent the mean \pm SEM (error bars) laboratory result value for the indicated group of data points. Panel C: $n = 87$ patients/paired albumin measurements, $n = 21$ patients/paired LDL measurements. Panel D: $n = 715$ patients/paired albumin measurements, $n = 20$ patients/paired LDL measurements. Statistical significance was determined using paired Student's t tests. Graphs and statistics were generated using GraphPad Prism.

Figure 6: In panels B, C, and D, each data point represents $n = 1$ independent humanized mouse. Horizontal lines represent the mean \pm SEM (error bars) of the indicated measurement/ratio for the indicated treatment group. Statistical significance was determined using unpaired Student's t tests. Graphs and statistics were generated using GraphPad Prism.

Supplemental Information

**A Drug Screen using Human iPSC-Derived
Hepatocyte-like Cells Reveals Cardiac Glycosides
as a Potential Treatment for Hypercholesterolemia**

Max A. Cayo, Sunil K. Mallanna, Francesca Di Furio, Ran Jing, Lauren B. Tolliver, Matthew Bures, Amanda Urick, Fallon K. Noto, Evanthia E. Pashos, Matthew D. Greseth, Maciej Czarnecki, Paula Traktman, Wenli Yang, Edward E. Morrisey, Markus Grompe, Daniel J. Rader, and Stephen A. Duncan

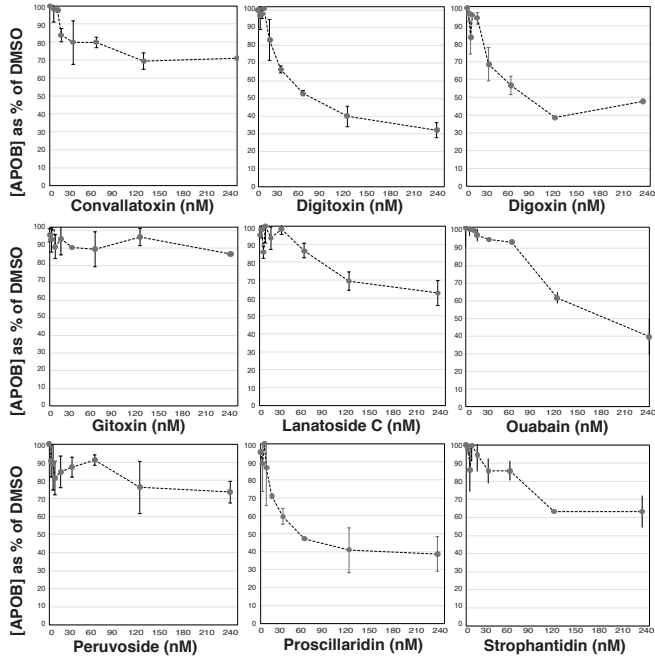


Figure S1. Related to Figure 3. Dose response curves of the effect of cardiac glycosides on APOB by iPSC–derived hepatocyte–like cells. Graphs showing dose response curves generated from the treatment of hepatocyte-like cells derived from wild type K3 iPSCs with various cardiac glycosides at 1, 5, 20, 78, 312, 1250, and 5000 nM. Error bars represent standard error of the mean across 3 biological replicates.

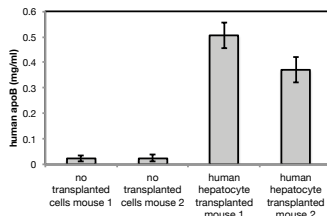
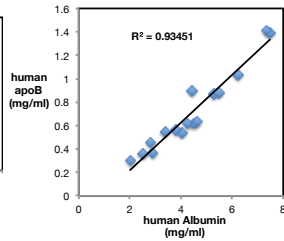
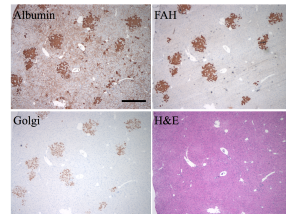
A**B****C**

Figure S2. Related to Figure 6 and STAR Methods.

Human apoB and Albumin can be measured in FRGN mice repopulated with human hepatocytes. (A) Bar graph showing that an antibody against human apoB specifically detects human apoB by ELISA in the serum of FRGN mice transplanted with human hepatocytes, but not in control FRGN mice. (B) Graph showing that the level of human apoB closely correlates with the level of human Albumin in the sera of humanized mice over time. (C) Repopulation of FRGN mice by primary human hepatocytes after long term cycling of NTBC. At 12 weeks post-transplant, clusters of primary human hepatocytes can be found within the parenchyma of FRGN mice. Human hepatocytes can be detected (brown) in serial sections by immunostaining with antibodies to detect human Albumin, FAH, and a human protein within the trans-golgi network TGN46 (Golgi). H&E staining reveals that the morphology of the liver is normal, indicating that the human cells have engrafted into the parenchyma. This mouse had a human serum albumin level of 865 $\mu\text{g}/\text{ml}$ at the time of analysis. Only mice with human serum Albumin levels with $>1 \text{ mg}/\text{ml}$ were used for drug trials. Scale bar = 500 μm . Error bars = SEM across 3 technical replicates.

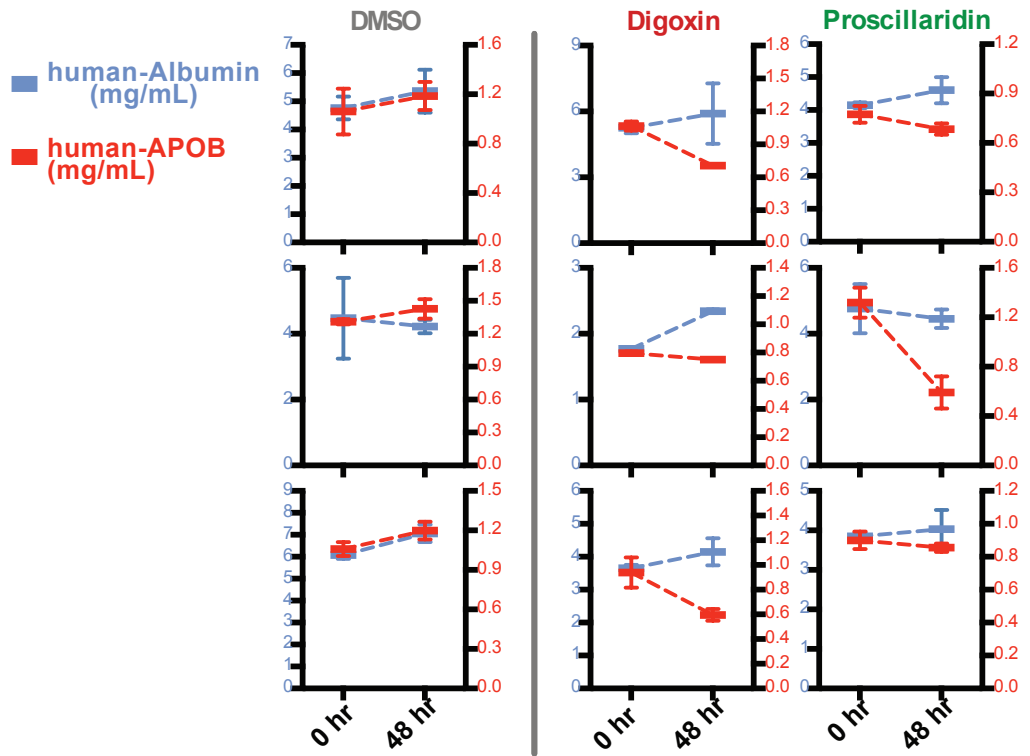


Figure S3. Related to Figure 6 and STAR Methods Section

Effect of cardiac glycosides on serum levels of human APOB and Albumin in individual humanized FRGN mice. Graphs depict the serum concentrations of human APOB (Red) and human Albumin (Blue) in individual avatar mice before and after treatment with (DMSO) Vehicle, Digoxin, or Proscillaridin over a 48-hour period. Error bars equal SEM measured across 3 technical replicates.

Table S1. Related to Figure 1. Drug Screen Data. List of all drugs screened in the SPECTRUM collection and the corresponding z-score of changes in APOB in the medium of iPSC–derived hepatocytes after treatment.